Transportation Geotechnics 30 (2021) 100627

Contents lists available at ScienceDirect

Transportation Geotechnics

journal homepage: www.elsevier.com/locate/trgeo

Application of hybrid intelligent systems in predicting the unconfined compressive strength of clay material mixed with recycled additive

Mohammed Ali Mohammed Al-Bared [a], Zahiraniza Mustaffa [b], Danial Jahed Armaghani [c,*], Aminaton Marto [d,g], Nor Zurairahetty Mohd Yunus [e], Mahdi Hasanipanah [f,*]

[a] Department of Civil and Environmental Engineering, Universiti Teknologi Petronas, 32610 Bandar Seri Iskandar, Malaysia
[b] Department of Civil and Environmental Engineering, Universiti Teknologi Petronas, 32610 Bandar Seri Iskandar, Malaysia
[c] Department of Urban Planning, Engineering Networks and Systems, Institute of Architecture and Construction, South Ural State University, 76, Lenin Prospect, Chelyabinsk 454080, Russian Federation
[d] Malaysia-Japan International Institute of Technology, Universiti Teknologi Malaysia (UTM) Kulala Lumpur, 54100 Kulala Lumpur, Malaysia
[e] Department of Geotechnics and Transportation, School of Civil Engineering, Faculty of Engineering, Universiti Teknologi Malaysia, 81310 UTM Johor Bahru, Johor, Malaysia
[f] Institute of Research and Development, Duy Tan University, Da Nang 550000, Vietnam
[g] Research Center for Soft Soil, Universiti Tun Hussein Onn, Malaysia

ARTICLE INFO

Keywords:
Soil treated-based material
Unconfined compressive strength
Neuro-swarm
Neuro-imperialism
Optimization

ABSTRACT

A reliable prediction of the soil properties mixed with recycled material is considered as an ultimate goal of many geotechnical laboratory works. In this study, after planning and conducting a series of laboratory works, some basic properties of marine clay treated with recycled tiles together with their unconfined compressive strength (UCS) values were obtained. Then, these basic properties were selected as input variables to predict the UCS values through the use of two hybrid intelligent systems i.e., the neuro-swarm and the neuro-imperialism. Actually, in these systems, respectively, the weights and biases of the artificial neural network (ANN) were optimized using the particle swarm optimization (PSO) and imperialism competitive algorithm (ICA) to get a higher accuracy compared to a pre-developed ANN model. The best neuro-swarm and neuro-imperialism models were selected based on several parametric studies on the most important and effective parameters of PSO and ICA. Afterward, these models were evaluated according to several well-known performance indices. It was found that the neuro-swarm predictive model provides a higher level of accuracy in predicting the UCS of clay soil samples treated with recycled tiles. However, both hybrid predictive models can be used in practice to predict the UCS values for initial design of geotechnical structures.

Introduction

Nowadays, the availability of suitable foundation soil with desirable geotechnical properties for civil engineering structures is considered very low due to the increased demand for development and industrialization [1]. Insufficient resources, increase of population, shortage in energy, and land scarcity are the main factors resulting in tremendous construction development setbacks [2]. Hence, the demand is increased for the reclamation of soft and marine soils which are considered problematic for construction activities. Soft soils are widely spread around the world and when this kind of soil is encountered, soil improvement is a must in order to meet the engineering requirements. Soft soils are associated with high plasticity and instability, high compressibility and void ratio, low shear strength and natural moisture content that is higher than the liquid limit [3–7]. The traditional most common methods used to stabilize/improve soft soils are the mechanical and chemical methods that are in use since the past century. Soil is improved mechanically by compaction and chemically using chemical additives such as ordinary Portland cement (OPC), lime, sodium and magnesium silicate, etc. [8–16]. The chemical additives significantly enhanced the strength and the other properties of soils, but the extent of improvement is dependent on the type of soil, natural moisture content, soil mineralogy, environmental condition, curing time, and type of chemical additive used [17]. Although those traditional additives were

* Corresponding authors.
E-mail addresses: mohammed_17005214@utp.edu.my (M.A.M. Al-Bared), zahiraniza@utp.edu.my (Z. Mustaffa), danialarmaghani@susu.ru (D.J. Armaghani), aminaton@utm.my (A. Marto), nzurairahetty@utm.my (N.Z.M. Yunus), hasanipanahmahdi@duytan.edu.vn (M. Hasanipanah).

https://doi.org/10.1016/j.trgeo.2021.100627
Received 14 January 2021; Received in revised form 1 April 2021; Accepted 13 July 2021
Available online 21 July 2021

able as demonstrated by the literature to improve the properties of soft soils, but there are many concerns that were recently raised regarding the use of chemical additives. They are considered harmful to the surrounding environment, costly, require advanced instruments during the application at site, and may pollute the underground water [18].

Currently, researchers in the field of geotechnical and coastal engineering are looking for stabilization additives/methods that are sustainable, economical, environmentally friendly, and able to alter the mechanical characteristics of problematic soils [19–23]. Rouaiguia and Abd El Aal [24] used marble waste and lime to enhance the geotechnical properties of soft soil in Algeria. The results revealed an increase in the unconfined compressive strength (UCS) of the soil with the increase of curing time and the percentages of marble waste and lime. The optimum marble content was 6% at which the strength was the highest. Besides, the optimum moisture content (OMC) was decreased with a corresponding increase in the maximum dry density (MDD) of the treated soil. In addition, Saygili [25] utilized waste marble dust in various percentages to stabilize problematic clayey soil. The results showed that the shear strength parameters of the treated soil were improved, and the swelling potential was significantly reduced. Sarkar et al. [26] utilized the waste of rice to treat the geotechnical properties of clayey soil. The properties of soil were modified by the treatment and the UCS value was improved. Mirzababaei et al. [27] utilized the waste of carpet fibers to stabilize clayey soils. The results showed that the UCS of samples prepared using the same dry density and optimum moisture content was significantly improved by the inclusion of the carpet fibers as additive and the mode of failure was found to be ductile. Moreover, Li et al. [28] used polypropylene fiber and fly ash to improve the mechanical properties of soil. The inclusion of the fly ash and the polypropylene fiber had a positive effect on the UCS, and 30% fly ash and 1% fiber were found to be the optimum content.

In general, the determination of the geotechnical properties of soft soils requires energy, time, labor, equipment, and high cost. For example, to determine the compaction parameters and the UCS of soil, at least six and four tests, respectively must be done in order to obtain reliable values. Hence, to evaluate the compaction parameters, UCS and the other parameters of soil in an efficient manner, prediction models were constructed to address this issue. However, the accuracy of predication was not very accurate for large data sets and therefore machine learning (ML) techniques were employed for high accuracy prediction models for most of the soil parameters [29–34]. Motamedi et al. [2] used the adaptive neuro-fuzzy inference system (ANFIS) to predict the UCS value of treated sand with cement and pulverized fuel ash. To enable the accuracy of the predication, series of laboratory tests were conducted for checking and training. The results indicated that for the prediction of the UCS value, the ANFIS root mean square error (RMSE) value was 0.0617. Soleimani et al. [35] used a multi-gen genetic programming (MGGP) to predict the UCS value of clayey soil treated with geopolymer. Several parameters that have direct effect on the UCS of soil such as plasticity index, plastic limit, percentages of additives, and others were incorporated within the proposed MGGP model. Parametric study was also conducted to validate the results and the models used. The results indicated a good accuracy of the equations used in the evaluation of the UCS. Moreover, Mozumder et al. [36] used 213 samples of soil treated with geopolymer based additive for the prediction of the shear strength using the support vector machine regression (SVR). The outcome of the study revealed the ability of the SVR to accurately predict the shear strength of the geopolymer treated soil. Kalkan et al. [37] developed ANFIS and artificial neural network (ANN) models for the prediction of the UCS value of compacted granular soil. A total of 64 UCS experimental samples were used to train the ANFIS and ANN models and about 20 experimental samples were used for the prediction of the UCS value. The results obtained from both models were compared and those of ANFIS model were more encouraging. Güllü and Fedakar [38] used various artificial intelligence (AI) techniques to estimate the UCS value of soil treated with bottom ash, jute fiber and steel fiber. The results obtained from all the employed AI techniques were significantly correlated with the measured UCS value of soil. In addition, Cabalar et al. [39] reviewed the application of ANFIS in geotechnical engineering such as triaxial testing and triggers for liquefaction. The results of the conducted critical review showed that ANFIS was successfully used in the prediction of the UCS value, friction angle of soil, stability of tunnels, induced depth around the group piles, and the permeability of soils. For instance, the compaction parameters of soil (maximum dry density and optimum moisture content) were predicted using multi expression programming (MEP). The optimal setting for the MEP code was proposed after collecting numerous compaction tests with different compaction energies and soil classification to form a large database. The results of the model showed the ability of the model to predict the compaction parameters for the various types of soils involved within the database and with a very high accuracy. It should be mentioned that the successful use of AI and ML models has been highlighted in many studies related to science and engineering [40–67].

Several studies have been conducted using PSO and imperialist competitive algorithm (ICA) in estimating the geotechnical properties of soil and rock with high accuracy and minimal deficiencies [68–71]. Dehghanbanadaki et al. [72] used two types of computational methods to predict the UCS of stabilized peat soil. A total of 271 samples were tested at different dosages of additives in the laboratory to develop a model for the UCS prediction. The model predicted the UCS of the treated peat soil through two types of ANN models that were trained using particle swarm optimization (ANN-PSO) and back propagation (ANN-BP) algorithms. Sensitivity analysis was carried out to evaluate the influence of each input on predicting the output and two performance indices were examined. The results revealed that ANN-PSO model better estimated the UCS compared to the ANN-BP model. On the other hand, Ray et al. [73] found that minimax probability machine regression (MPMR) outperformed ANN-PSO and ANN-ANFIS in predicting the settlement of shallow foundations on soils. Armaghani et al. [74] developed hybrid ANN-PSO model that is able to predict the ultimate bearing capacity of rock socketed piles. When compared with other conventional ANN for predicting the ultimate bearing capacity, the developed hybrid model showed higher degree of accuracy. A study was conducted by Pham et al. [75] to develop a prediction model for the undrained shear strength of soil using the results of 127 samples as database for training and validating models. Pearson correlation coefficient (R) was utilized to compare and examine the developed model with the single RF model. The results revealed a high accuracy ($R = 0.89$) of the developed model in predicting the undrained shear strength and was found to be superior when compared with the single RF model. Kutanaei and Choobbasti [76] performed a series of laboratory tests to evaluate the UCS of sand treated with cement and polyvinyl alcohol (PVA) fiber. The results were also used to develop a polynomial model based on PSO to predict the UCS, axial strain and modulus of elasticity of the treated soil. The performance of the developed model was compared with the results obtained from the laboratory and was found to have good agreement. Moreover, Armaghani et al. [77] developed a hybrid model based on ANN enhanced with ICA able to estimate the unconfined compressive strength and the Young's modulus of rock. The model was trained using experimental results, and it was compared with a conventional ANN predictive model. The performance indices indicated that the predicted UCS and Young's modulus using the ANN-ICA model were of high degree of accuracy. Tian et al. [78] developed a hybrid model based on PSO and ICA to solve the shortcomings of the ANN itself when predicting the Young's modulus of rock. The developed model was trained and tested, and the results showed good accuracy.

In this present study, the UCS of marine clay (MC) treated with recycled tiles (RT) is estimated by developing two hybrid ANN models namely particle swarm optimization (PSO)-ANN and neuro-swarm and imperialism competitive algorithm (ICA)-ANN or neuro-imperialism. In another words, the index properties, compaction parameters, percentage of recycled tiles, and curing time were used as inputs in the proposed

ANN-based models to estimate the UCS of treated marine soil. The rest of this paper is organized as follows:

Section "Need for research" explain and discuss the problem statement and the need for conducting this research. Section "Intelligent models principles" presents the background of the used intelligence techniques in this study together with the used statistical indices for evaluating intelligence techniques. Then, in Section "Laboratory investigations and established database", the details of laboratory tests and the way of selecting input parameter are described. The intelligence modelling of the hybrid models in predicting the UCS values of soil material is given in Section "Intelligent modelling and assessment". Afterward, Sections "Discussion" and "Conclusions" are about discussions and conclusions of the study, respectively.

Need for research

Soft soil is normally treated mechanically by compaction, chemically using the various chemical additives, biologically using bacteria, or hydrologically using hydrants. The treatment using chemicals is very efficient and the most used, but several adverse impacts by those chemicals on the ecosystem made it the last choice for soil treatment. Recently, scientists and researchers are looking for a cost effective, environmentally friendly and sustainable material that can alter and enhance the properties of the soil. Therefore, there is a need to utilize the available waste materials to treat soft soils economically and in environmental-friendly manner. In this research, the waste of ceramic tiles is utilized as an environmentally friendly material to treat soft marine clay. Besides, conducting several laboratory tests to evaluate the strength of soils is found to be very costly, time consuming, requires materials, equipment, and presence in the laboratory. Hence, this present study is focused to estimate the strength of marine clay treated with recycled tiles (RT) by developing two hybrid ANN models namely particle swarm optimization (PSO)-ANN and neuro-swarm and imperialism competitive algorithm (ICA)-ANN or neuro-imperialism.

Intelligent models principles

Artificial neural network

Artificial neural network (ANN) can be described as a computing system built to interpret the way the human beings' brain processes and evaluates data for the purpose of developing an artificial system. The ANN-based models can accurately and automatically predict relationships between the input and output information by making a possible use of input training patterns. This feature makes those models have big difference in functionality compared with any other models available in this field [79]. The artificial neurons are employed as basic units by the ANN models to process data in a parallel manner like that of a biological brain. McCulloch and Walter [80] attempted for the first time to model the neural network and successfully modelled an effective artificial neurons' behavior by assembling a binary decision unit. Their system was able to obtain outputs of higher correctness by allocating the artificial node with the total weight of an input signal and applied an activating function to those signals. Ch and Mathur [81] explained that ANN system is a network of nodes that are interconnected and found in an exceptional parallel layer in a computing system. Their outcome shows that the neuron connection patterns highly influence the class and behavior of those networks.

The ANN functions can be divided from a structure point of view into two classifications named as feedback and feed forward. Multilayer perceptron (MLP) is considered the most popular among those that fall under the feed forward multi-layer networks. MLP is responsible for processing the existing data using the activation functions within back-to-back layers. Besides, Simpson [82] introduced the learning algorithm known as the back propagation (BP) which usually helps the network to learn by making use of a learning procedure-based gradient. BP that is comprised of a twofold training cycle can produce an acceptable outcome for the networks that are formed of a feed-forward multilayer [83]. The twofold training cycle is a forward and a backward stage. The operation of each stage was explained in detail in some relevant investigations conducted by other scholars [84]. Those scholars showed that the input signals proceed forward in each phase and transfer error signal for each node found in the output layer. This is followed by the resultant error rates moving backwards and this is how the weights and biases of network are changed. Generally, several activation functions are applied to the input to produce the neuron's output. After that, the outputs will be transferred as an input to the neuron found in the next layer. Meanwhile, the difficulty of the problem dealing with will determine the kind of activation function. As a result, sigmoid transfer functions (log or tangent sigmoid) may be employed when encountering non-linear situations. Fig. 1 shows a systematic diagram for an artificial node *j*.

Particle swarm optimization

Particle swarm optimization (PSO) was introduced as an optimization technique for the first time by Kennedy and Eberhart [85]. The idea of this computational technique was inspired from the simplified social systems such as fish swarms that is similar to the nonlinear procedure contained within PSO. It involves particles that are repetitively searching for optimal values/targets. During the search stage, the positions of the particles will be altered by using the particles' gained experiences and those other particles found in the system. The particle is trained to reach its best position by following two personal and global positions; the best personal position (PBEST) and the best global position (GBEST). Each particle is trained during the processes of the learning stage to accelerate aiming towards its own PBEST and GBEST positions. To achieve this, the distance of each particle from its own PBEST and GBEST positions will be used as a basis for the calculation of new velocity term. Hence, the new position of the particle in the following iteration will depend on the new value of the velocity. For the purpose of achieving the value of the updated velocity and movement of the particle, Eqs. (1) and (2), respectively are employed within the PSO. To be more precise, Eq. (1) is used to calculate the actual movement of the particle through its specific velocity vector whereas Eq. (2) is employed to direct the provided velocity vector into its own PBEST and GBEST.

$$\overrightarrow{v_{new}} = \overrightarrow{v} + C_1 \times \left(\overrightarrow{pbest} - \overrightarrow{p}\right) + C_2 \times \left(\overrightarrow{gbest} - \overrightarrow{p}\right) \quad (1)$$

$$\overrightarrow{p_{new}} = \overrightarrow{p} + \overrightarrow{v_{new}} \quad (2)$$

In which, $\overrightarrow{v_{new}}$ refers to the updated velocity of the particle, $\overrightarrow{v}$ stands for the current velocity of the particle, $\overrightarrow{p_{new}}$ determines the new position of the particle, $\overrightarrow{p}$ signifies the current position of the particle, C_1 and C_2 are pre-specified coefficient, and $\overrightarrow{pbest}$ and $\overrightarrow{gbest}$ denote the personnel and global best positions of the particle. Meanwhile, there are many research papers published in the literature which provided more detailed explanation of the PSO and its structure [86]. Fig. 2 demonstrates a detailed flowchart for the PSO.

Imperialist competitive algorithm

The imperialist competitive algorithm (ICA) was pioneered by Atashpaz-Gargari and Lucas [87] to be implemented in solving the different problems of optimization. The algorithm used in the ICA is based on population and it is utilized for the global search to find the optima and the rate of convergence. The operation in ICA starts by random initial population solution, while the initial population solution in other optimization algorithms (OAs), such as PSO, is comprised of individuals that are named as particles and chromosomes, respectively. In ICA, the individuals are referred to as countries and the best countries

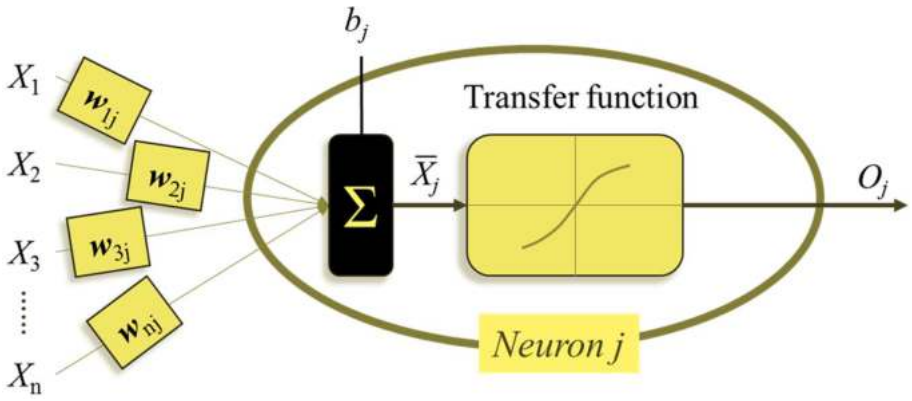

Fig. 1. Mathematical model for the artificial neuron.

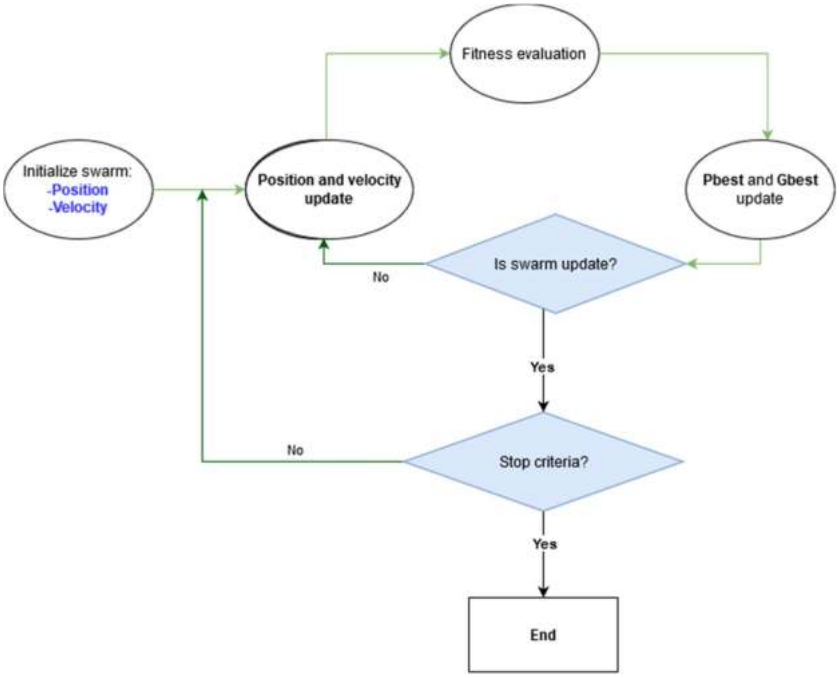

Fig. 2. Detailed flowchart for the algorithm of PSO [85].

of the highest power are identified as imperialists. While the remainder of the countries in the scenario of ICA are described as colonies of the imperialists. The design of the ICA originally follows the real socio-politic competition at which the imperialists in the real world normally compete each other trying to control or take the colonies. The most powerful countries in the ICA algorithm are those that are associated with the least cost and will have the ability to take the ownership of more colonies. The ICA is usually consisted of three main operators called as assimilation, revolution, and competition. The role of the assimilation operator is to guide the colonies to grow into imperialists in order to gain more power and control, obtain better cultural level and improved economy. The colonies get a good chance during the assimilation and revolution operators to reach a position that is better than their respective imperialists and this will result in the colonies taking the control of the empire. On the contrary, during the competition operator, the imperialists will have great opportunities to adopt more and more colonies. This process will result in every empire trying to possess other empire's colonies by force. Hence, every imperialist will be able to adopt at least one colony that has been adopted by the weakest empire and this will entirely depend on their power. The weakest empire will be totally collapsed by the competition operator processes, while the strongest empires will be able to have more colonies which will result in increasing their power to the most possible level. This process will be repeated until only one strongest empire will survive and take control, and all the other weak empires will be collapsed and changed into colonies. Meanwhile, the available literature demonstrated more details and explanation for the applications of the ICA [87,88]. The processes of ICA from the beginning until the end are illustrated in Fig. 3.

Hybrid models

The capabilities of the ANN models were improved by employing the OAs such as PSO, genetic algorithm, and ICA by many scholars working in the field of engineering and sciences [89,90]. It is probably possible for the ANN models to obtain a wrong or objectionable prediction due to the weak ability of BP models in exploring the global minimum in an unacceptable accuracy [91]. ANN models have high possibility of giving strong local minima when generating the algorithms, but the optimization algorithms can overcome this situation by determining the weight and biases of the ANN. Hence, the space of searching in this case will face the global minimum due to the usage of the OAs. In this condition, the ANN model will be the determining factor of the most logical

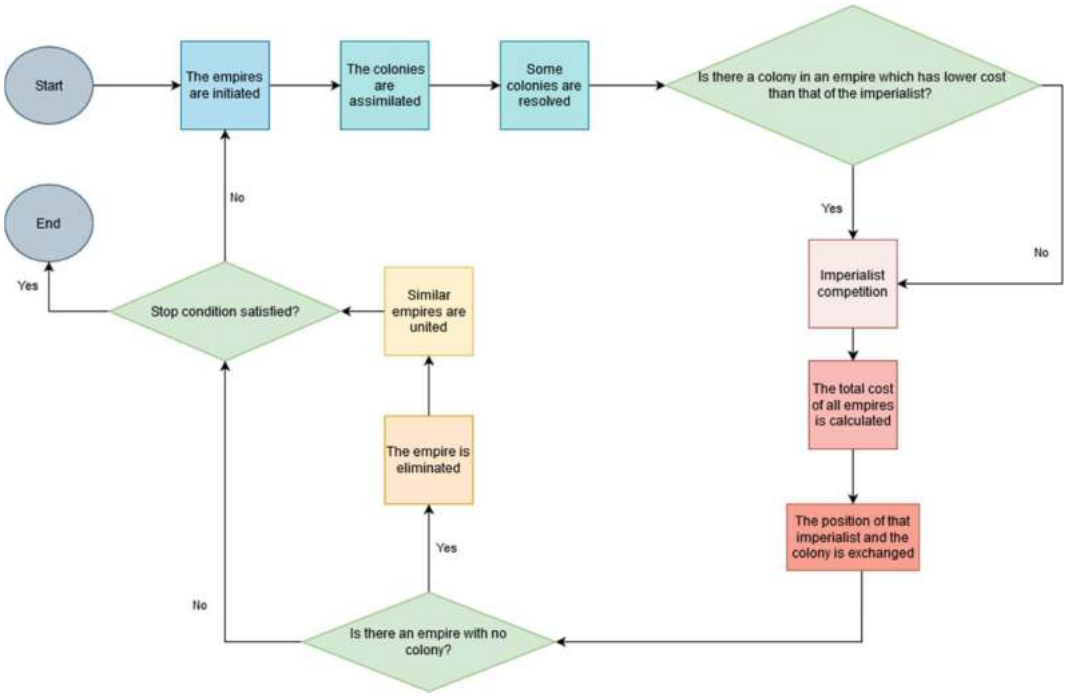

Fig. 3. Flow chart illustrating the structure and algorithm of ICA.

outcomes obtained by the hybrid ANN based models. This study used two hybrid ANN-based models (i.e., PSO-ANN, and ICA-ANN) for the prediction of the UCS of treated soil. This is followed by comparing the prediction results obtained by both hybrid ANN-based models in order to choose the best model among those. Figs. 4 and 5 show the ways of combinations of ANN model with ICA and PSO OAs which can be used for prediction purposes.

Performance index

The performance index of the hybrid ANN-based models is normally evaluated by performing calculation of two different statistical parameters named as root mean square error (RMSE) and the determination's coefficient (R^2). When the values of RMSE are low, this indicate that the predication is good and accurate. While for the R^2, the higher value represents a good agreement between the measured and the estimated

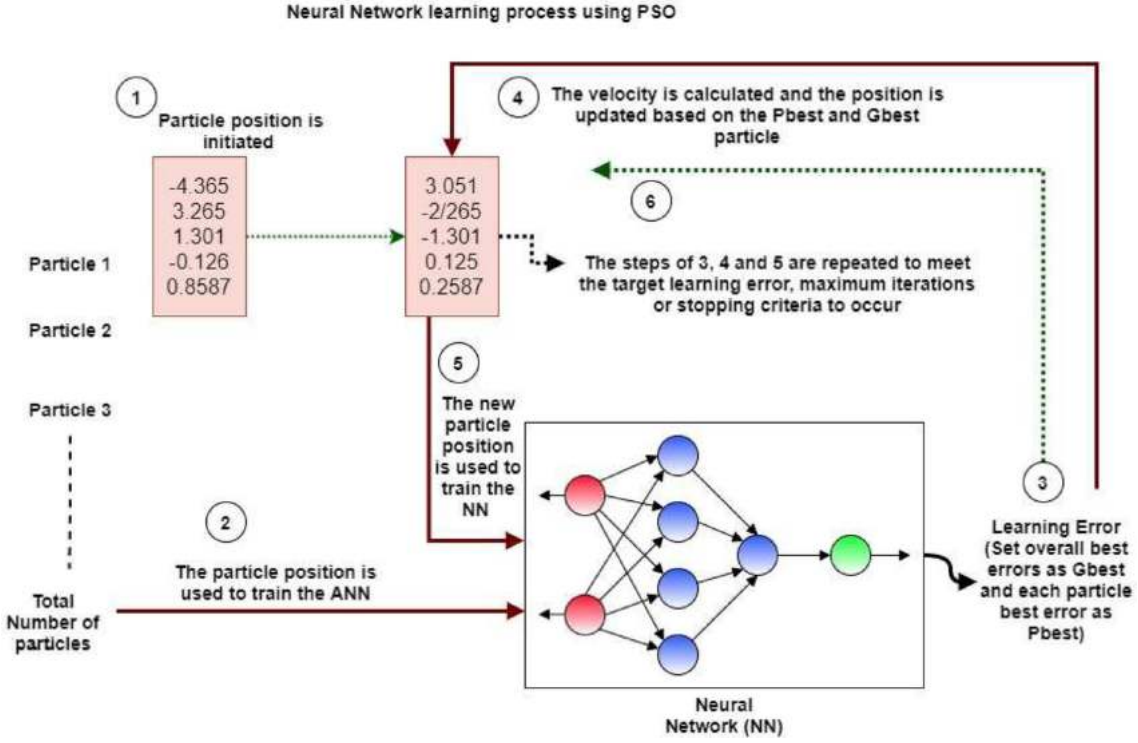

Fig. 4. Neuro-swarm flowchart.

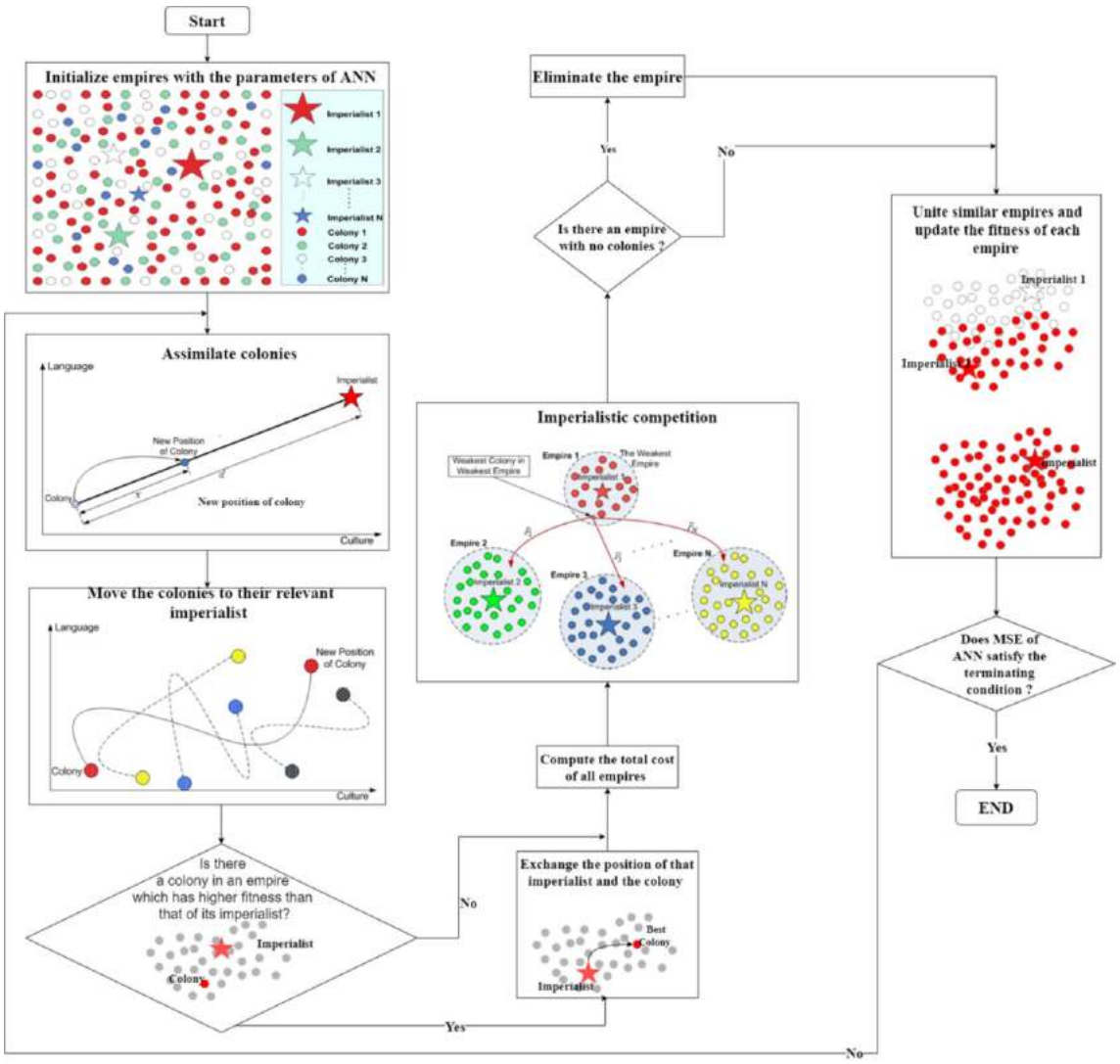

Fig. 5. Neuro-imperialism flowchart.

values. The following Eqs. (3) and (4) show the calculation of these statistical parameters mentioned earlier:

$$\mathrm{RMSE} = \sqrt{\frac{1}{n}\sum_{i=1}^{n}(x_i - y_i)^2} \tag{3}$$

$$R^2 = 1 - \left(\frac{\sum_{i=1}^{n}(x_i - y_i)^2}{\sum_{i=1}^{n}(x_i - \overline{x})^2}\right) \tag{4}$$

where the total number of databases is represented by the symbol n and the estimated and targeted values are respectively denoted by x_i and y_i.

The R^2 and RMSE were used in the evaluation of the accuracy and consistency of the developed neutral networks. The RMSE is usually implemented in presenting short term data that is considered a guideline to show the difference between the predicted data and the one obtained during the laboratory testing. When obtaining a low RMSE value, this indicates a good and precise evaluation. On the other hand, the interpreted variation by the model is evaluated with the R^2 that can be the decrease in variation while employing the model. The value of R^2 is measured in the range from zero to one and the good analyzing capability of the model is observed when the value of R^2 is near one and the capability is reduced when approaching zero.

Laboratory investigations and established database

Material properties

The materials used in this research are the problematic MC and the waste of RT. MC is a soft soil collected from Nusajaya, Johor, Malaysia. Few steps were followed for preparing the soil for experiments; MC was cleaned from plants and roots, air-dried, grinded and sieved through 2 mm sieve size before being stored in an airtight plastic container. On the other hand, RT were collected from construction site in Taman Pelangi, Johor Malaysia that was observed to have plenty of waste for this material. Tiles were first cleaned to remove all the foreign materials sticking on their surface, crushed manually into small pieces by hammer, crushed further using machine into a mixture containing particles of less than 5 mm diameter size, and blended into a fine size using Los Angeles abrasion machine. The mechanical shaker was used to separate the mixture of tiles into the selected sizes. The macro-structural properties of MC and RT are listed in Table 1 after Al-Bared et al. [92,93].

Conducted laboratory tests

The untreated and treated specimens of MC underwent the Atterberg limits tests to observe the changes induced by the treatment on their index properties. The specimens of MC were passed through a sieve size

Table 1
Physical and mechanical properties of MC and RT [93].

No.	Property	MC	RT
1	Phase	Powder	Powder
2	Size (mm)	Less than 2 mm	Between 0.063 and 0.30 mm
3	Texture	Fine	Fine and coarse
4	Liquid limit (%)	41	–
5	Plastic limit (%)	12	–
6	Plasticity index (%)	19	–
4	pH	2.8	9
	G_s	2.52	2.56
7	MDD (Mgm^{-3})	1590	–
8	OMC (%)	22	–
9	UCS (kPa)	50	–
10	Dominant minerals	Quartz	Silica and Aluminum dioxide

of 0.425 mm and then mixed with 10, 20, 30, and 40% 0.063, 0.15 and 0.30 mm RT in a dry condition. The mixture of MC and RT was admixed with distilled water and remained inside airtight plastic bag for 24 h to make sure the moisture content is properly distributed within the mixture. The sample preparation and testing were performed in accordance with the BS 1377, part 2 [94]. Fig. 6 shows the test set up for the Atterberg limits.

Compaction tests were carried out on untreated and treated MC specimens to examine the size and percentage influence of RT on the compaction parameters. A compaction mold with diameter and height of 105 and 115.5 mm, respectively was used for the determination of MDD and OMC. The untreated MC specimen was oven dried, sieved through 2 mm mesh, mixed with the appropriate dried percentage and size of RT, and thoroughly stirred with the anticipated amount of distilled water. The preparation of specimens and testing methods followed the BS 1377, part 4 [95].

The UCS specimens for both untreated and treated MC were prepared using the predetermined values of MDD and OMC obtained from the compaction tests. The specimens were remolded inside a triaxial mold with a dimension of 80 mm height and 38 mm diameter. A total of 12 specimens were used to evaluate the UCS of untreated MC at 0, 7, 14, and 28 days curing periods. While for the treated specimens, the MC was first mixed with 10, 20, 30, and 40% of 0.063, 0.15 and 0.30 mm RT until homogeneity was observed. Then, an equal amount of the predetermined OMC was added and mixed thoroughly with MC and RT. The wet mix was put into the triaxial mold in three equal layers and compacted each for 27 blows. A hydraulic jack machine was used to extrude the cylindrical specimens and the specimens were trimmed using a knife. The specimens were then put inside airtight plastic bags and stored in humidity chamber (97% humidity and temperature of 27 °C) for the required curing period. The UCS testing was conducted on 156 untreated and treated specimens under strain-controlled condition at which the strain was set at 1.52 mm per minute. The specimens preparation and the methods of testing were in accordance with the BS 1377, part 4 [96].

Fig. 6. Liquid limit sample and apparatus.

Results of laboratory investigations

The results of the compaction, pH, Atterberg limits, and UCS tests for both untreated and treated clay specimens are listed in Table 2. The Table shows the UCS value as an output while all other influencing parameters were presented as inputs. Fig. 7 shows the effect of MDD on the UCS value of the treated specimens using different sizes and proportions of the RT additive. The UCS value was significantly affected by the increase of the MDD of treated specimens. It was increased with the increased MDD until reaching a peak value and then slightly started to drop. The size of the additive also influenced the UCS value and the smallest micro size resulted with greater UCS value than other sizes. On the other hand, the effect of the decrease in the OMC was increasing the UCS value of the treated specimens as shown in Fig. 8. The treatment resulted in decreasing the OMC and therefore the UCS of the specimens was increased for all the utilized sizes of the additive. As observed with MDD, the micro size of RT had the most influencing effect compared with bigger sizes.

The pH value of the treated specimens using different sizes of RT is plotted in Fig. 9 to reveal the extent of pH impact on the UCS value. The decrease in the pH value of the treated specimens was corresponded with an increase in the UCS value until approaching maximum value at which the UCS value started to decline. In addition, Fig. 10 shows the effect of the additive percentage and size and the curing period on the UCS value of the treated specimens. The percentage of RT played a significant role in either increasing or decreasing the UCS value of the treated specimens. For specimens cured for 28 days, higher percentages of RT resulted in higher UCS value until reaching the optimum percentage and then declined. The optimum RT percentage for 0.063, 0.15 and 0.3 mm was 20, 30 and 40%, respectively. The size of RT contributed to increase the UCS value and 0.3 mm indicated the highest value of UCS. However, 0.063 mm size attained almost similar UCS value with lower percentage of RT compared to 0.3 mm. Hence, 0.063 mm is considered to be the optimum size from environmental and economical point of view.

Input selection

To develop a generic model that would be able to predict the UCS value of untreated and treated clay soil, various percentages and sizes of additive, curing time, and other influencing parameters are considered. The index and mechanical parameters such as the liquid limit, plastic limit, plasticity index, MDD, OMC, and pH are observed to have a great influencing effect on the prediction of UCS. The liquid limit of clayey soils is always correlated with the soil's behavior due to the importance of this parameter. The inter particle cementation of clayey soils is indicated using the liquidity index. The significance of the pH value is reflected during the stabilization/treatment processes of clayey soils as it controls the cementation reaction. When the pH value is high, better stabilization can be achieved as this will help to dissolve the existing silica and alumina within the soil to react with the calcium forming calcium silicate hydrates and calcium aluminum hydrates. Moreover,

Table 2
Laboratory data used in the estimation of the UCS of untreated and treated MC.

Input parameter								Output
Mixture	% of RT	Size of RT (mm)	Curing Time (days)	MDD kg m-3	OMC (%)	pH	PI (%)	UCS (kPa)
UMC	0	0	0	1.59	22	2.89	19	50
UMC	0	0	0	1.59	22	2.89	19	50
UMC	0	0	0	1.59	22	2.89	19	52
UMC	0	0	7	1.59	22	2.89	19	50
UMC	0	0	7	1.59	22	2.89	19	50
UMC	0	0	7	1.59	22	2.89	19	50
UMC	0	0	14	1.59	22	2.89	19	50
UMC	0	0	14	1.59	22	2.89	19	50
UMC	0	0	14	1.59	22	2.89	19	50
UMC	0	0	28	1.59	22	2.89	19	50
UMC	0	0	28	1.59	22	2.89	19	50
UMC	0	0	28	1.59	22	2.89	19	50
TMC	10	0.063	0	1.66	19	2.73	18.27	75
TMC	10	0.063	0	1.66	19	2.73	18.27	80
TMC	10	0.063	0	1.66	19	2.73	18.27	85
TMC	10	0.063	7	1.66	19	2.73	18.27	133
TMC	10	0.063	7	1.66	19	2.73	18.27	143
TMC	10	0.063	7	1.66	19	2.73	18.27	137
TMC	10	0.063	14	1.66	19	2.73	18.27	180
TMC	10	0.063	14	1.66	19	2.73	18.27	181
TMC	10	0.063	14	1.66	19	2.73	18.27	178
TMC	10	0.063	28	1.66	19	2.73	18.27	200
TMC	10	0.063	28	1.66	19	2.73	18.27	202
TMC	10	0.063	28	1.66	19	2.73	18.27	199
TMC	20	0.063	0	1.67	19	2.69	15.54	80
TMC	20	0.063	0	1.67	19	2.69	15.54	88
TMC	20	0.063	0	1.67	19	2.69	15.54	85
TMC	20	0.063	7	1.67	19	2.69	15.54	133
TMC	20	0.063	7	1.67	19	2.69	15.54	142
TMC	20	0.063	7	1.67	19	2.69	15.54	137
TMC	20	0.063	14	1.67	19	2.69	15.54	210
TMC	20	0.063	14	1.67	19	2.69	15.54	217
TMC	20	0.063	14	1.67	19	2.69	15.54	219
TMC	20	0.063	28	1.67	19	2.69	15.54	223
TMC	20	0.063	28	1.67	19	2.69	15.54	217
TMC	20	0.063	28	1.67	19	2.69	15.54	222
TMC	30	0.063	0	1.72	18	2.65	15.59	114
TMC	30	0.063	0	1.72	18	2.65	15.59	109
TMC	30	0.063	0	1.72	18	2.65	15.59	110
TMC	30	0.063	7	1.72	18	2.65	15.59	136
TMC	30	0.063	7	1.72	18	2.65	15.59	138
TMC	30	0.063	7	1.72	18	2.65	15.59	143
TMC	30	0.063	14	1.72	18	2.65	15.59	155
TMC	30	0.063	14	1.72	18	2.65	15.59	154
TMC	30	0.063	14	1.72	18	2.65	15.59	152
TMC	30	0.063	28	1.72	18	2.65	15.59	156
TMC	30	0.063	28	1.72	18	2.65	15.59	159
TMC	30	0.063	28	1.72	18	2.65	15.59	161
TMC	40	0.063	0	1.73	16.5	2.61	12.84	116
TMC	40	0.063	0	1.73	16.5	2.61	12.84	118
TMC	40	0.063	0	1.73	16.5	2.61	12.84	121
TMC	40	0.063	7	1.73	16.5	2.61	12.84	125
TMC	40	0.063	7	1.73	16.5	2.61	12.84	110
TMC	40	0.063	7	1.73	16.5	2.61	12.84	120
TMC	40	0.063	14	1.73	16.5	2.61	12.84	137
TMC	40	0.063	14	1.73	16.5	2.61	12.84	134
TMC	40	0.063	14	1.73	16.5	2.61	12.84	129
TMC	40	0.063	28	1.73	16.5	2.61	12.84	158
TMC	40	0.063	28	1.73	16.5	2.61	12.84	158
TMC	40	0.063	28	1.73	16.5	2.61	12.84	159
TMC	10	0.15	0	1.7	18	2.7	13.94	97
TMC	10	0.15	0	1.7	18	2.7	13.94	96
TMC	10	0.15	0	1.7	18	2.7	13.94	99
TMC	10	0.15	7	1.7	18	2.7	13.94	111
TMC	10	0.15	7	1.7	18	2.7	13.94	124
TMC	10	0.15	7	1.7	18	2.7	13.94	127
TMC	10	0.15	14	1.7	18	2.7	13.94	160
TMC	10	0.15	14	1.7	18	2.7	13.94	170
TMC	10	0.15	14	1.7	18	2.7	13.94	168
TMC	10	0.15	28	1.7	18	2.7	13.94	180
TMC	10	0.15	28	1.7	18	2.7	13.94	177
TMC	10	0.15	28	1.7	18	2.7	13.94	186
TMC	20	0.15	0	1.71	18	2.68	13.15	98

(*continued on next page*)

Table 2 (*continued*)

Input parameter								Output
Mixture	% of RT	Size of RT (mm)	Curing Time (days)	MDD kg m-3	OMC (%)	pH	PI (%)	UCS (kPa)
TMC	20	0.15	0	1.71	18	2.68	13.15	100
TMC	20	0.15	0	1.71	18	2.68	13.15	96
TMC	20	0.15	7	1.71	18	2.68	13.15	158
TMC	20	0.15	7	1.71	18	2.68	13.15	160
TMC	20	0.15	7	1.71	18	2.68	13.15	166
TMC	20	0.15	14	1.71	18	2.68	13.15	190
TMC	20	0.15	14	1.71	18	2.68	13.15	191
TMC	20	0.15	14	1.71	18	2.68	13.15	190
TMC	20	0.15	28	1.71	18	2.68	13.15	192
TMC	20	0.15	28	1.71	18	2.68	13.15	194
TMC	20	0.15	28	1.71	18	2.68	13.15	190
TMC	30	0.15	0	1.74	17.8	2.67	11.82	98
TMC	30	0.15	0	1.74	17.8	2.67	11.82	111
TMC	30	0.15	0	1.74	17.8	2.67	11.82	102
TMC	30	0.15	7	1.74	17.8	2.67	11.82	158
TMC	30	0.15	7	1.74	17.8	2.67	11.82	172
TMC	30	0.15	7	1.74	17.8	2.67	11.82	170
TMC	30	0.15	14	1.74	17.8	2.67	11.82	204
TMC	30	0.15	14	1.74	17.8	2.67	11.82	200
TMC	30	0.15	14	1.74	17.8	2.67	11.82	188
TMC	30	0.15	28	1.74	17.8	2.67	11.82	205
TMC	30	0.15	28	1.74	17.8	2.67	11.82	199
TMC	30	0.15	28	1.74	17.8	2.67	11.82	201
TMC	40	0.15	0	1.74	17	2.64	12.76	122
TMC	40	0.15	0	1.74	17	2.64	12.76	134
TMC	40	0.15	0	1.74	17	2.64	12.76	128
TMC	40	0.15	7	1.74	17	2.64	12.76	146
TMC	40	0.15	7	1.74	17	2.64	12.76	135
TMC	40	0.15	7	1.74	17	2.64	12.76	132
TMC	40	0.15	14	1.74	17	2.64	12.76	172
TMC	40	0.15	14	1.74	17	2.64	12.76	175
TMC	40	0.15	14	1.74	17	2.64	12.76	165
TMC	40	0.15	28	1.74	17	2.64	12.76	182
TMC	40	0.15	28	1.74	17	2.64	12.76	181
TMC	40	0.15	28	1.74	17	2.64	12.76	179
TMC	10	0.3	0	1.69	19	2.78	13.99	118
TMC	10	0.3	0	1.69	19	2.78	13.99	124
TMC	10	0.3	0	1.69	19	2.78	13.99	122
TMC	10	0.3	7	1.69	19	2.78	13.99	149
TMC	10	0.3	7	1.69	19	2.78	13.99	161
TMC	10	0.3	7	1.69	19	2.78	13.99	154
TMC	10	0.3	14	1.69	19	2.78	13.99	157
TMC	10	0.3	14	1.69	19	2.78	13.99	171
TMC	10	0.3	14	1.69	19	2.78	13.99	163
TMC	10	0.3	28	1.69	19	2.78	13.99	205
TMC	10	0.3	28	1.69	19	2.78	13.99	195
TMC	10	0.3	28	1.69	19	2.78	13.99	203
TMC	20	0.3	0	1.67	16.7	2.75	12.65	135
TMC	20	0.3	0	1.67	16.7	2.75	12.65	126
TMC	20	0.3	0	1.67	16.7	2.75	12.65	129
TMC	20	0.3	7	1.67	16.7	2.75	12.65	166
TMC	20	0.3	7	1.67	16.7	2.75	12.65	154
TMC	20	0.3	7	1.67	16.7	2.75	12.65	159
TMC	20	0.3	14	1.67	16.7	2.75	12.65	166
TMC	20	0.3	14	1.67	16.7	2.75	12.65	162
TMC	20	0.3	14	1.67	16.7	2.75	12.65	158
TMC	20	0.3	28	1.67	16.7	2.75	12.65	206
TMC	20	0.3	28	1.67	16.7	2.75	12.65	197
TMC	20	0.3	28	1.67	16.7	2.75	12.65	200
TMC	30	0.3	0	1.75	16.5	2.72	12.42	134
TMC	30	0.3	0	1.75	16.5	2.72	12.42	138
TMC	30	0.3	0	1.75	16.5	2.72	12.42	132
TMC	30	0.3	7	1.75	16.5	2.72	12.42	165
TMC	30	0.3	7	1.75	16.5	2.72	12.42	166
TMC	30	0.3	7	1.75	16.5	2.72	12.42	163
TMC	30	0.3	14	1.75	16.5	2.72	12.42	178
TMC	30	0.3	14	1.75	16.5	2.72	12.42	180
TMC	30	0.3	14	1.75	16.5	2.72	12.42	168
TMC	30	0.3	28	1.75	16.5	2.72	12.42	229
TMC	30	0.3	28	1.75	16.5	2.72	12.42	224
TMC	30	0.3	28	1.75	16.5	2.72	12.42	222
TMC	40	0.3	0	1.77	15	2.7	10.57	134
TMC	40	0.3	0	1.77	15	2.7	10.57	135
TMC	40	0.3	0	1.77	15	2.7	10.57	136

(*continued on next page*)

Table 2 (*continued*)

Input parameter								Output
Mixture	% of RT	Size of RT (mm)	Curing Time (days)	MDD kg m-3	OMC (%)	pH	PI (%)	UCS (kPa)
TMC	40	0.3	7	1.77	15	2.7	10.57	176
TMC	40	0.3	7	1.77	15	2.7	10.57	170
TMC	40	0.3	7	1.77	15	2.7	10.57	165
TMC	40	0.3	14	1.77	15	2.7	10.57	232
TMC	40	0.3	14	1.77	15	2.7	10.57	222
TMC	40	0.3	14	1.77	15	2.7	10.57	225
TMC	40	0.3	28	1.77	15	2.7	10.57	237
TMC	40	0.3	28	1.77	15	2.7	10.57	230
TMC	40	0.3	28	1.77	15	2.7	10.57	225

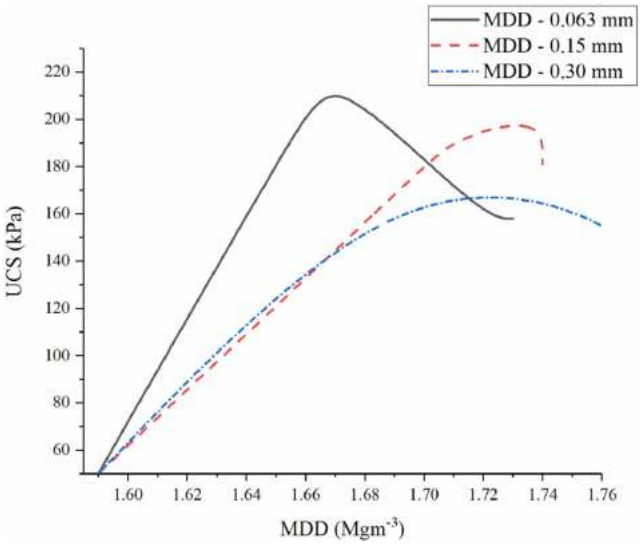

Fig. 7. Impact of MDD on the value of UCS of treated MC.

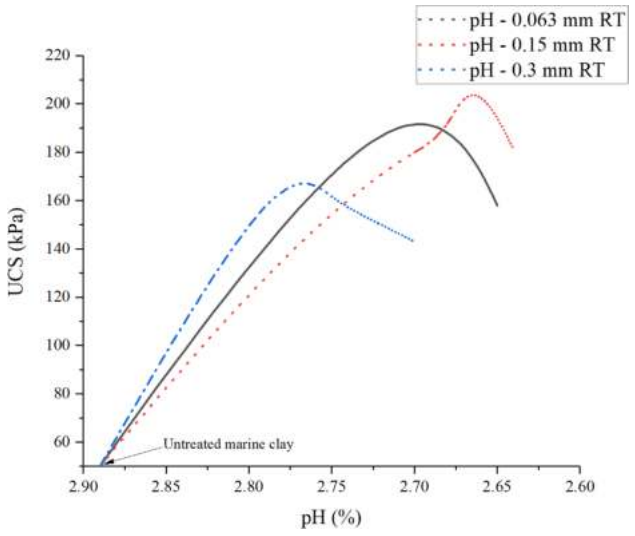

Fig. 9. Influence of pH on the value of UCS of treated MC using different sizes of RT.

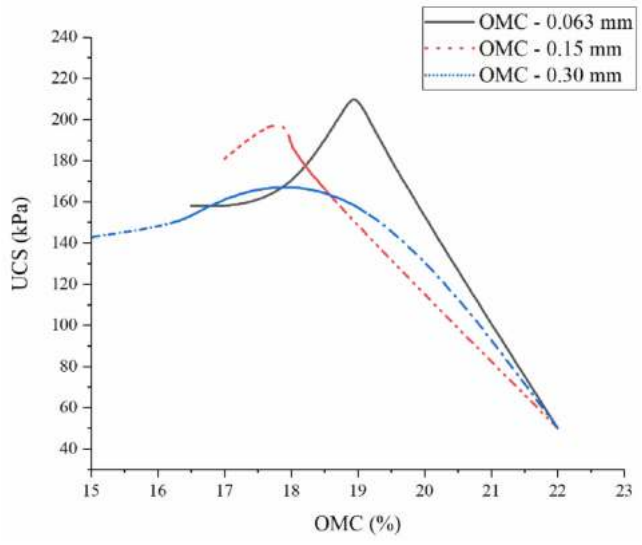

Fig. 8. Impact of OMC on the value of UCS of improved specimens.

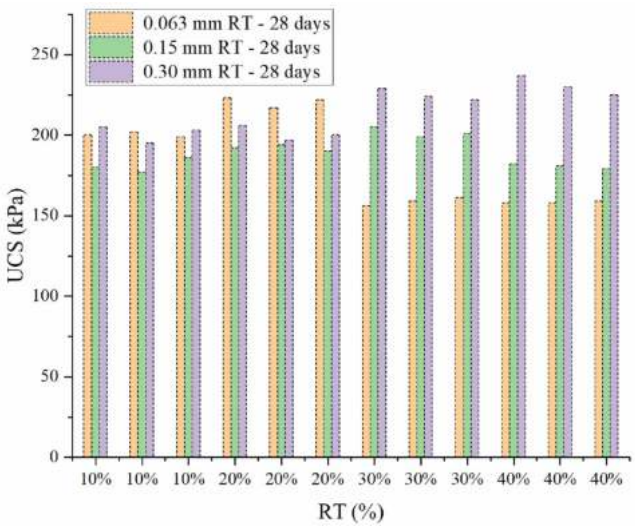

Fig. 10. Effect of inclusion of different percentages and sizes of RT on the UCS value of MC.

the compaction parameters of soil play an important role in predicting the UCS value of clayey soils. The reduction of OMC would definitely result in increasing the UCS value of the treated clay specimens as the affinity of soil molecules to absorb water is reduced when the soil is improved. Besides, the MDD of soil reflects the unit weight at which the soil is approximately free from air voids and the soil particles are intact or very close to each other. Therefore, the MDD control the strength and stiffness of soil and affect the stabilization of soil. When MDD and OMC of soil are high and low, respectively, the chances for better improvement are increased.

The prediction of the UCS value for untreated and treated soils usually depends highly on the influencing soil parameters as reported by many recent studies. For instance, the prediction of the UCS value of

treated soil was investigated by Motamedi et al. [2] using the curing time and the percentage of additives. In addition, Soleimani et al. [35] used the factors of liquid limit, plastic limit, plasticity index, percentage and concentration of additives for the prediction of the UCS value of soil treated with geopolymer. Narendra et al. [17] used parameters such as liquid limit (LL), liquidity index (LI), pH and sodium ion concentration (Na^{+}) for the prediction of the UCS value of soft grounds.

Intelligent modelling and assessment

Modelling

Neuro-swarm model

The modelling stages should be started by determining the most influential parameters of the ANN system itself. However, before that, the data should be normalized. A certain equation was suggested by Liou et al. [91] for the normalization of the datasets at the beginning of the modelling process in a way to make the following process simplified:

$$X_{norm} = (X - - X_{min}) / (X_{max} - X_{min}) \quad (5)$$

where, minimum and maximum values of X are denoted by X_{min} and X_{max}, respectively, X is the measured value, and X_{norm} signifies the normalized value.

Some researchers suggested using only one hidden layer in ANN [79,97,98] and some others proposed an ANN model with more than one hidden layer for solving their problems [99,100]. Therefore, we examined hidden layers of one, two and three on our data to predict the UCS of treated marine soil. The results of this parametric study (PS) showed that one hidden layer can receive more accurate prediction performance compared to other implemented numbers. The number of neurons is another important factor in ANN performance that should be determined using another PS. According to previous studies, values of 5, 6, 7, 8, 9, 10, 11, 12, 13, 14, and 15 were considered and used in the modelling of this part where their RMSE values were evaluated. From these analyses, it was found that the hidden neuron number of 10 provides closer UCS values to the measured ones and due to that this value was selected for the best ANN model. Therefore, based on results of these PSs, a model with seven input variables, 10 hidden neurons and one output neuron as the best ANN model is introduced and the rest of modelling in this research is conducted with this model as reference in part of ANN. It is worth noting that a combination of 80–20% of the total number of data samples was selected and used in this study as training and testing datasets, respectively.

In the neuro-swarm modelling, the first stage involves the selection of swarm size and number of iterations at the same time. With the help of PS, the swarm size was set to a range from 50 to 500 with the incremental step of 50, and the maximum number of iterations was set to 500. As a result, 10 neuro-swarm predictive models were configured for the purpose of predicting the UCS value of the treated marine soil on the basis of RMSE given in Fig. 11. To do these analyses, in initial iterations, the RMSE values were considerably reduced for all models; after that, the alteration of the values was minimized gradually until reaching a constant value. As depicted in Fig. 11, the minimum error was achieved in the case where the swarm size was fixed at 450. In addition, it can be clearly observed that RMSE reached to a constant value after 300 iterations. Therefore, for the modelling purposes in the present paper, the swarm size and the number of iterations were fixed at 450 and 300, respectively, in order to predict the UCS of the treated marine soil.

Then, in the second stage, the C_1 and C_2 parameters are determined. Similar to the former stages, PS was implemented with a range of C_1 and C_2 values to explore the best suited to our model. To this end, the neuro-swarm models were constructed with the following setting: ($C_1 = 2$ and $C_2 = 2$), ($C_1 = 1.5$ and $C_2 = 1.5$), ($C_1 = 1{,}75$ and $C_2 = 1.75$), ($C_1 = 2$ and $C_2 = 1.5$), ($C_1 = 1.5$ and $C_2 = 2$), and ($C_1 = 2.5$ and $C_2 = 2.5$). RMSE and R^2 were taken into consideration as the criteria for evaluating the predictive performance of the models (see Table 3). As confirmed by the results given in Table 3, the velocity coefficients have significant effects on the neuro-swarm models because the results significantly differ from one combination to another. Though, it is not easy to select the optimal model just by considering PIs since, as can be observed, there are only small differences among the relevant statistics. To cope with this challenge, the present paper makes use of a simple ranking approach introduced by Zorlu et al. [101] in which each neuro-swarm model can be graded separately on the basis of its capacity of training and testing data sets. The best PI within this ranking system receives the highest rank, 6, whereas the worst one is assigned with the lowest rank. As shown by the assigned entire rank scores given in Table 3, amongst the six neuro-swarm models designed in this study, the first model (or No. 1) with the ranking of 23 was found the most efficient model in terms of accuracy in predicting UCS. As a result, both C_1 and C_2 were set to 2 and applied to the last modelling part, which was dedicated to determining the inertia weight (IW). This parameter in all models was fixed at 0.25.

Another parameter with a high impact on the neuro-swarm models is IW that, more specifically, affects the accuracy level of these models [102]. Consequently, the values of 0.25, 0.5, 0.75, and 1 were set for this parameter in the four neuro-swarm models presented in this paper. Table 4 presents the results obtained by this setting. The ranking system was implemented on these PIs in both training and testing phases. Based on the total rank values (i.e., 16, 8, 8, and 8), among all, Model 1 with IW

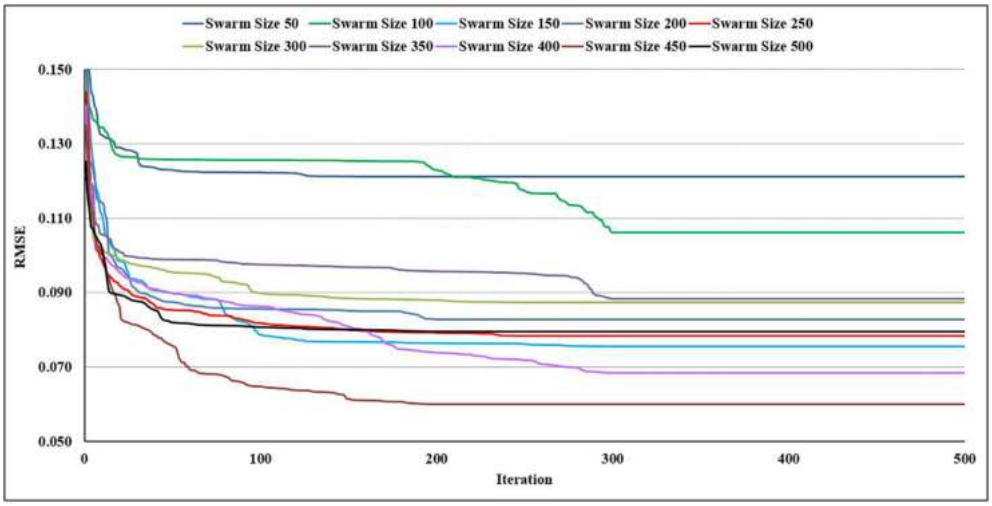

Fig. 11. A simultaneous selection of both swarm size and number of iterations in predicting the UCS of treated marine soil.

Table 3
Six neuro-swarm models with different C_1 and C_2 values.

Stage	PIs	Model No. 1	Model No. 2	Model No. 3	Model No. 4	Model No. 5	Model No. 6
		$C_1 = 2, C_2 = 2$	$C_1 = 1.5, C_2 = 1.5$	$C_1 = 1.75, C_2 = 1.75$	$C_1 = 2, C_2 = 1.5$	$C_1 = 1.5, C_2 = 2$	$C_1 = 2.5, C_2 = 2.5$
Train	R^2	0.9345 Rank = 5	0.7774 Rank = 1	0.8929 Rank = 3	0.8301 Rank = 2	0.8985 Rank = 4	0.9371 Rank = 6
	RMSE	0.0601 Rank = 6	0.1106 Rank = 1	0.0819 Rank = 3	0.1024 Rank = 2	0.0798 Rank = 4	0.0646 Rank = 5
Test	R^2	0.9556 Rank = 6	0.7321 Rank = 1	0.8307 Rank = 3	0.7921 Rank = 2	0.8813 Rank = 4	0.9147 Rank = 5
	RMSE	0.0641 Rank = 6	0.1575 Rank = 1	0.1021 Rank = 3	0.1172 Rank = 2	0.0827 Rank = 4	0.0648 Rank = 5
Total Rank		23	4	12	8	16	21

Table 4
Four neuro-swarm models with different IW values.

Stage	PIs	Model No. 1	Model No. 2	Model No. 3	Model No. 4
		IW = 0.25	IW = 0.5	IW = 0.75	IW = 1
Train	R^2	0.9345	0.8992	0.9087	0.9178
		Rank = 4	Rank = 1	Rank = 2	Rank = 3
	RMSE	0.0601	0.0784	0.0739	0.0705
		Rank = 4	Rank = 1	Rank = 2	Rank = 3
Test	R^2	0.9556	0.9174	0.9063	0.8577
		Rank = 4	Rank = 3	Rank = 2	Rank = 1
	RMSE	0.0641	0.0742	0.0805	0.1006
		Rank = 4	Rank = 3	Rank = 2	Rank = 1
Total Rank		16	8	8	8

of 0.25 and the total rank of 16 demonstrated the highest capacity for fitting the measured and predicting UCS values. For that reason, the mentioned neuro-swarm model was chosen as the optimal model obtained from 3 PSs. Its accuracy level in the prediction of UCS of the treated marine soil is discussed later in detail.

Neuro-imperialism model

Here, the modelling steps taken by the neuro-imperialism technique to estimate the UCS values of treated marine soil are described. As mentioned earlier, three parameters, i.e., the number of IMPs, number of decades, and number of countries, significantly affect the performance capacity of the neuro-imperialism model. Therefore, there is need to design these parameters and achieve the optimum values for the parameters with the use of different PSs. To simultaneously select the numbers of countries and decades, the first PS was carried out. For that purpose, comparable to the former section and on the basis of a number of previously-conducted studies [58,103], in the first PS, the number of countries was ranged between 50 and 500 with incremental step of 50, and the maximum number of decades was fixed at 500. Fig. 12 presents the results obtained from various numbers of countries based on their number of decades in terms of the prediction of the UCS value of the treated marine soil. As the figure clearly depicts, most of the numbers of countries are converged in RMSE values in the range of 0.09–0.11. When the number of countries was fixed at 350, the minimum RMSE was obtained. In addition, when the number of decades was fixed at 350, no more reduction was observed in RMSE. As a result, this value was chosen as the optimum number of decades applicable to modelling the neuro-imperialism model.

Up to this point, the optimal numbers of countries and decades were determined; now, it is the time to execute another PS to determine the best value of the number of IMPs. To do this, IMP was ranged from 5 to 10. Table 5 presents the results obtained by this PS on the basis of R^2, RMSE and the ranking system. The R^2 values ranging from 0.8 to 0.95 were obtained for training and testing, respectively, which show a high efficiency of the neuro-imperialism models regarding the UCS prediction. The neuro-imperialism models of numbers 1 to 6 obtained the rank values of 14, 14, 19, 11, 16, and 10, respectively. It reveals the highest predictive capability of Model 3 (with IMP of 7). As a result, this model was chosen for the purpose of this study to estimate the UCS value of the treated marine soil. For this model, 350, 350 and 7 were obtained as the optimal values for the number of countries, number of decades and number of IMPs, respectively. The following section discusses this model and its obtained results.

Model assessment

In this sub-section, the results of the hybrid ANN-based models in the prediction of the UCS of the treated marine soil are discussed. Numerous PIs, as noted earlier, can be used for the aim of evaluating the prediction capability of a model. In this part, R^2 and RMSE were chosen to be computed for the developed models. The mentioned PIs were calculated

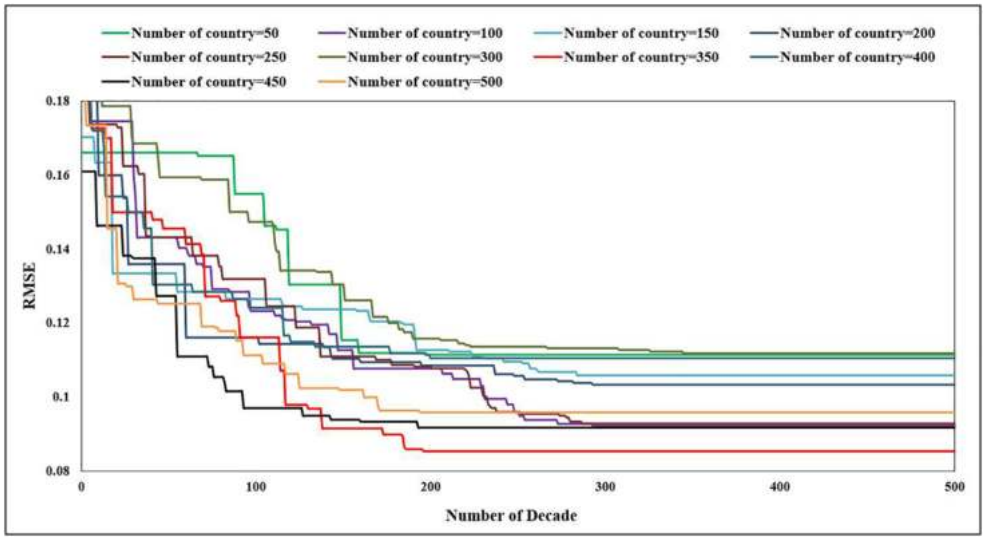

Fig. 12. A simultaneous selection of both No. of countries, No. of decades in predicting the UCS of treated marine soil.

Table 5
Six neuro-imperialism models with different IMP values.

Stage	PIs	Model No. 1	Model No. 2	Model No. 3	Model No. 4	Model No. 5	Model No. 6
		IMP = 5	IMP = 6	IMP = 7	IMP = 8	IMP = 9	IMP = 10
Train	R^2	0.8908 Rank = 6	0.8711 Rank = 5	0.8415 Rank = 3	0.8138 Rank = 1	0.8576 Rank = 4	0.8325 Rank = 2
	RMSE	0.0844 Rank = 6	0.0913 Rank = 5	0.0930 Rank = 4	0.1011 Rank = 2	0.0970 Rank = 3	0.1030 Rank = 1
Test	R^2	0.7979 Rank = 1	0.8218 Rank = 2	0.9538 Rank = 6	0.9042 Rank = 5	0.8735 Rank = 4	0.8568 Rank = 3
	RMSE	0.1023 Rank = 1	0.0958 Rank = 2	0.0574 Rank = 6	0.0942 Rank = 3	0.0784 Rank = 5	0.0913 Rank = 4
Total Rank		14	14	19	11	16	10

based on their formulas for the best neuro-swarm and neuro-imperialism models achieved within the former section.

Figs. 13–15 present the results of the neuro-swarm model and Figs. 13 and 14 depict the results of the calculated and estimated soil UCS values using the neuro-swarm model in both training and testing stages, respectively. Moreover, Fig. 15 illustrates the R^2 values of the training and testing stages of the developed neuro-swarm model. Figs. 16–18 demonstrate the same details for the neuro-imperialism model in the prediction of the UCS value of the treated marine soil.

Regarding the estimation capability, the hybrid neuro-swarm model was clearly capable of offering a better correlation between the measured and estimated UCS of the soil. In case of the training stage, the R^2 values of 0.8415 and 0.9345 for the neuro-imperialism and neuro-swarm models, respectively, revealed that the latter outperformed the other one in the model development stage. The results of an efficient model development stage can be observed in the testing stage as the R^2 values of 0.9538 and 0.9556 were achieved for the testing stage of and the neuro-imperialism and neuro-swarm models, respectively. The predicted and measured soil UCS values given in the mentioned figures show clearly the high capability of PSO in the optimization of the weights and biases of ANN. With appropriately optimizing the weights and biases of ANN, the performance capability of the neuro-swarm model could be higher than that of the neuro-imperialism model.

As well proved by the modelling process results, both the neuro-swarm and the neuro-imperialism models presented in the current paper are capable of accurately predicting the UCS values of soil. Nevertheless, when a new data is available, the neuro-swarm model was found more successful than the other one. Remember that the intelligent models developed in the current research are applicable with the same range of the input parameters used in the modelling process of this paper.

Discussion

During soil stabilization using cementitious or recycled based cementitious materials, the improvement in UCS value of soil is first indicated by the increase of the MDD and the decrease of OMC during compaction. In this study, the addition of the recycled ceramic in various percentages and sizes increased the MDD and reduced the OMC as illustrated in Figs. 7 and 8. The increase in MDD with the additions of additive is dependent on the particle size and specific gravity of RT at which the MC particles with low specific gravity and fineness were coated by RT particles of high specific gravity forming bigger aggregates that occupied larger spaces [104]. Whereas the reduction in OMC can be due to the decrease in the affinity of the MC particles to absorb higher quantities of water molecules. Similar results were obtained by various researchers who used cementitious/recycled based cementitious materials to treat soils [105]. The slight decrease in the pH value of the treated soil resulted in slight increase in acidity of treated soil. This slight increment in acidity of treated soil increased the free hydrogen ions (H^+) within the soil and increased the chances for soil reactions. Consequently, the UCS value was increased and the soil become more intact [18].

The sharp increase in the unconfined compressive strength of untreated MC by the addition of various percentages and sizes of RT could be due to the availability of high quantities of silica and alumina within MC and RT and also cementitious based minerals within RT such as calcium, sodium and magnesium. The silica and alumina react with the cementitious minerals to form new cementitious compounds such as sodium aluminum silicate and aluminum silicate hydrates responsible for the increased UCS value. As a result, the UCS value of the treated specimens was increased with the increased of curing time which allow the hydration and the pozzolanic reactions to be completed. When comparing the UCS results of the different sizes of RT, it is observed that the micro size (less than 0.063 mm) was the optimum size and the amount required of this size to achieve the highest strength was lower than the other sizes. Those results were in a close agreement with the limited available literature on improving the strength of soft soils using ceramic tile materials either in a crushed or powdered forms [106].

In terms of intelligence modelling, this study introduces two new

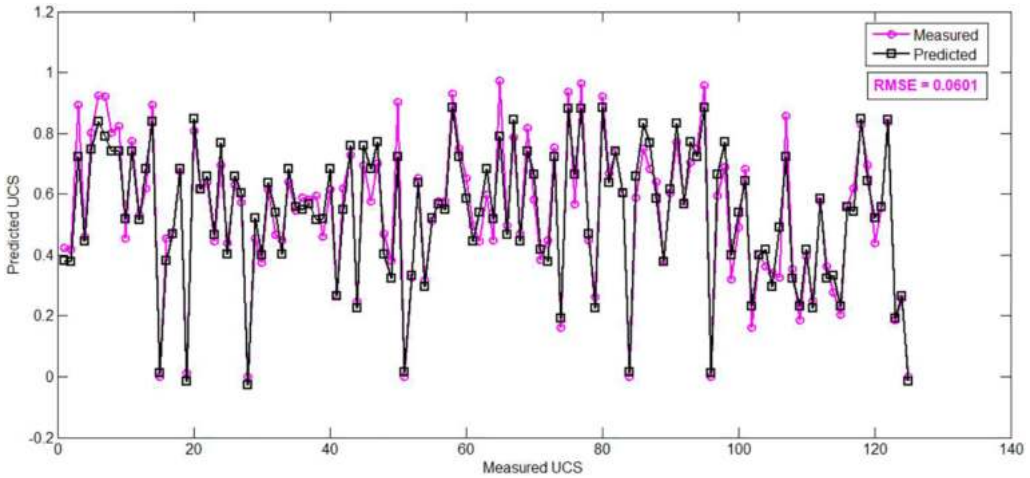

Fig. 13. Train stage results of the introduced neuro-swarm model in predicting the UCS of treated marine soil.

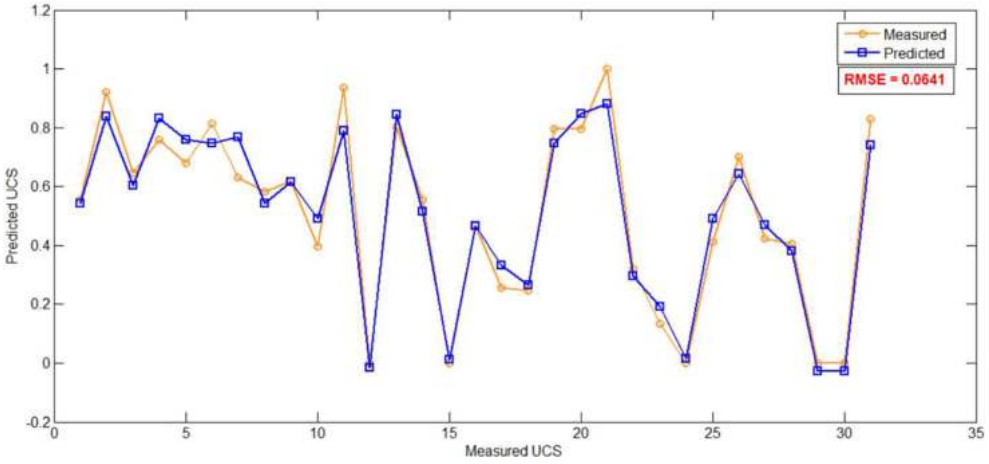

Fig. 14. Test stage results of the introduced neuro-swarm model in predicting the UCS of treated marine soil.

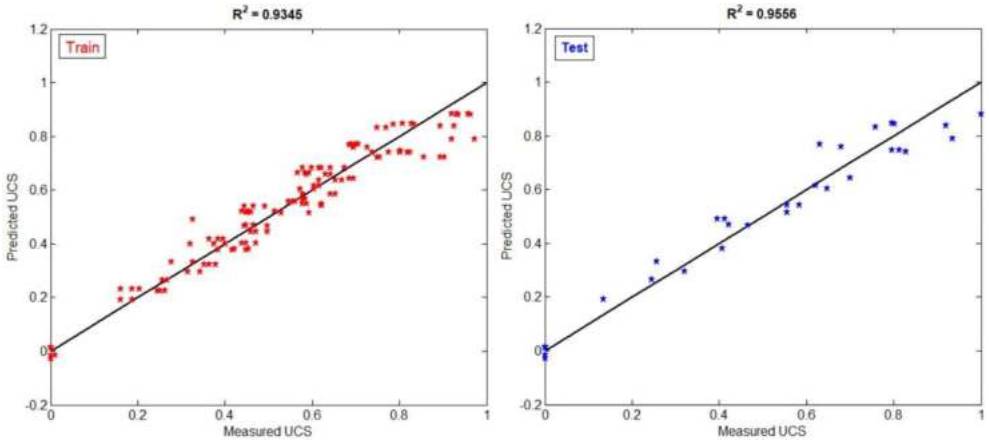

Fig. 15. R^2 values of the introduced neuro-swarm model.

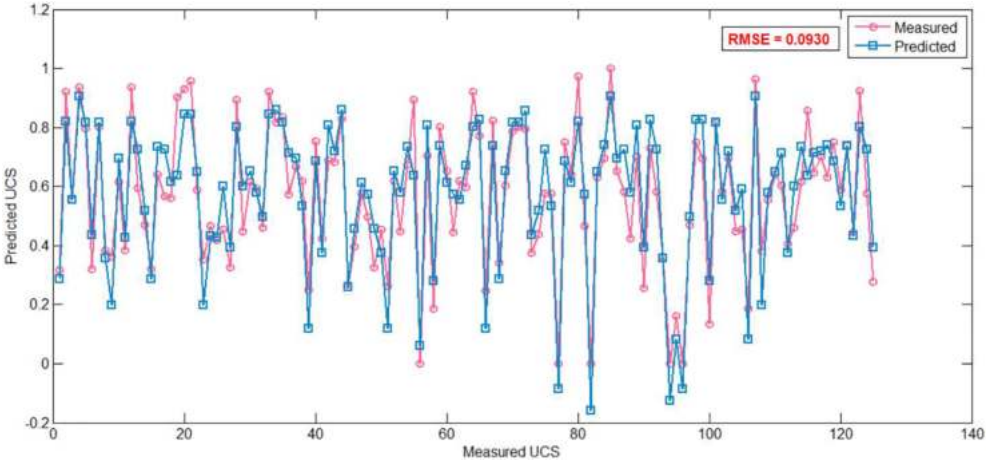

Fig. 16. Train stage results of the introduced neuro-imperialism model in predicting the UCS of treated marine soil.

hybrid ANN models namely neuro-swarm and neuro-imperialism models. These techniques are able to optimize ANN weights and biases to get a higher level of accuracy for prediction purposes using PSO and ICA OAs, respectively. After performing a series of PSs, the best neuro-swarm and neuro-imperialism models were selected to predict the UCS of treated marine soil. However, when considering system error, it is obvious that the PSO optimization algorithm is more powerful compared to the ICA technique. The optimum weights and biases of the ANN model cause the lowest system error in a hybrid ANN-based system. Therefore, RMSE values of (0.0601 and 0.0641) for training and testing datasets respectively, can be expected for the neuro-swarm model based on the above discussion. It can be expressed that to solve the defined problem related to the soil UCS prediction, the developed neuro-swarm (because of PSO optimization technique) model was found more

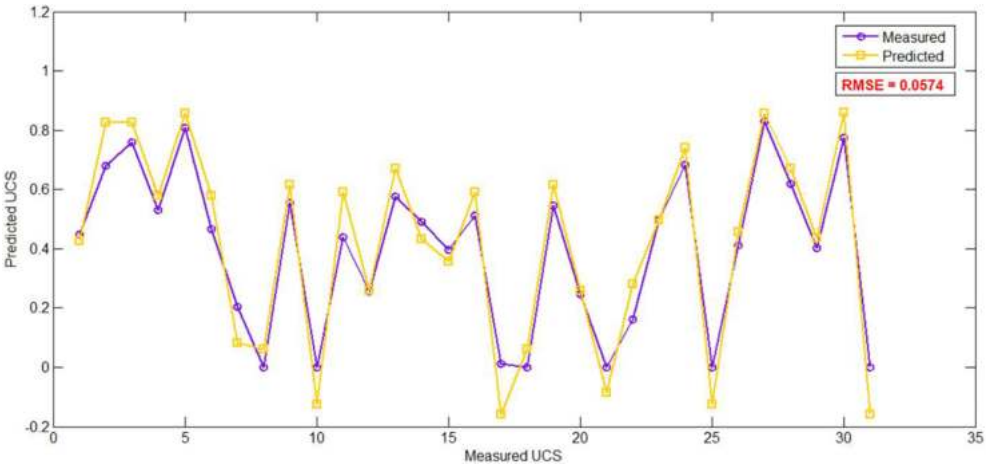

Fig. 17. Test stage results of the introduced neuro-imperialism model in predicting the UCS of treated marine soil.

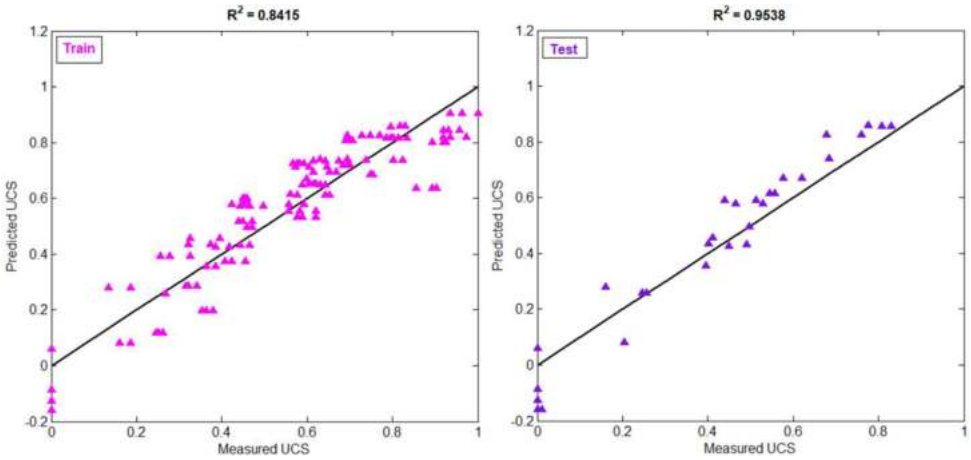

Fig. 18. R^2 values of the introduced neuro-imperialism model.

powerful and applicable compared to the developed neuro-imperialism model. Hence, the predicted soil UCS values obtained by the neuro-swarm model are more accurate than those obtained by the neuro-imperialism predictive technique. This study introduces the neuro-swarm (i.e., PSO-ANN) as a powerful and accurate model to solve soil UCS problem in the treated marine soil.

Conclusions

In this study, several laboratory tests were conducted such as liquid limit, plastic limit, pH, moisture content, compaction, and UCS to assess the behavior of untreated and RT-treated marine clay and to predict the UCS value of the samples. These tests were conducted according to the standards on remolded samples (38 mm diameter and 76 mm height) obtained from Nusajaya, Johor, Malaysia and prepared using different percentages and sizes of RT additive. This study was limited to remolded samples of marine clay of 80 mm height and 38 mm diameter. The findings of this research are drawn in the following conclusions:

- The measured UCS value of the RT-treated samples was improved with the increased of the curing time regardless of the material contents. The addition of the recycled additive resulted in decreasing the pH and the optimum moisture content of the improved soil while increasing the maximum dry density which significantly influenced the results of the UCS.
- The results of the hybrid ANN-based models used to predict the UCS of the treated marine clay samples showed that the neuro-swarm model was better than the neuro-imperialism model in model development stage. Results of a good attempt in model development stage can be seen in testing stage as R^2 values of 0.9556 and 0.9538 were obtained for testing stage of the neuro-swarm and the neuro-imperialism models, respectively.
- The proposed models can be used in initial design of geotechnical structures when soil strength value is required. The accuracy of the developed models is good enough for such projects. However, in order to develop models with a higher degree of accuracy, some newer optimization techniques such as gray wolf optimization, and moth flame optimization can be combined with ANN and ANFIS and fuzzy models for the UCS prediction.

CRediT authorship contribution statement

Mohammed Ali Mohammed Al-Bared: Writing - original draft, Methodology, Data curation. **Zahiraniza Mustaffa:** Conceptualization, Supervision. **Danial Jahed Armaghani:** Writing - original draft, Software, Supervision. **Aminaton Marto:** Writing - review & editing, Supervision. **Nor Zurairahetty Mohd Yunus:** Writing - review & editing, Supervision. **Mahdi Hasanipanah:** Writing - review & editing.

Declaration of Competing Interest

The authors declare that they have no known competing financial interests or personal relationships that could have appeared to influence the work reported in this paper.

Acknowledgements

This paper was premised on the research conducted using the Yayasan UTP Grant Scheme (015LC0-196) from Universiti Teknologi Petronas (UTP). The authors would like to express their sincere gratitude to UTP for its generous support.

References

[1] Alhani IJ, Md Noor MJ, Al-Bared MAM, Harahap ISH, Albadri WM. Mechanical response of saturated and unsaturated gravels of different sizes in drained triaxial testing. Acta Geotech 2020. https://doi.org/10.1007/s11440-020-00954-4.
[2] Motamedi S, Shamshirband S, Petković D, Hashim R. Application of adaptive neuro-fuzzy technique to predict the unconfined compressive strength of PFA-sand-cement mixture. Powder Technol 2015;278:278–85. https://doi.org/10.1016/j.powtec.2015.02.045.
[3] Al-Bared MAM, Marto A, Harahap ISH. Eco-friendly sustainable stabilization of dredged soft clay using low-carbone recycled additives. Foss Free Fuels Trends Renew Energy 2019:71–84.
[4] Kwon YM, Chang I, Lee M, Cho GC. Geotechnical engineering behavior of biopolymer-treated soft marine soil. Geomech Eng 2019;17:453–64. https://doi.org/10.12989/gae.2019.17.5.453.
[5] Wang L, Shen K, Ye S. Undrained shear strength of K0 consolidated soft soils. Int J Geomech 2008;8:105–13.
[6] Phetchuay C, Horpibulsuk S, Arulrajah A, Suksiripattanapong C, Udomchai A. Strength development in soft marine clay stabilized by fly ash and calcium carbide residue based geopolymer. Appl Clay Sci 2016;127–128:134–42. https://doi.org/10.1016/j.clay.2016.04.005.
[7] Al-Bared MAM, Marto A. A review on the geotechnical and engineering characteristics of marine clay and the modern methods of improvements. Malaysian J Fundam Appl Sci 2017;13:825–31.
[8] Yilmaz Y. Compaction and strength characteristics of fly ash and fiber amended clayey soil. Eng Geol 2015;188:168–77. https://doi.org/10.1016/j.enggeo.2015.01.018.
[9] Kunyong Z, Frederick CN. Important for correlation between compaction and Atterberg Limits characteristics of soils: aspects of clay content using artificial mixtures. KSCE J Civ Eng 2017;21:546–53.
[10] Al-Bared MAM, Marto A, Hamonangan IS, Kasim F. Compaction and plasticity comparative behaviour of soft clay treated with coarse and fine sizes of ceramic tiles. E3S Web Conf 2018;34:1–9. https://doi.org/10.1051/e3sconf/20183401012.
[11] Xiao H, Lee FH, Chin KG. Yielding of cement-treated marine clay. Soils Found 2014;54:488–501. https://doi.org/10.1016/j.sandf.2014.04.021.
[12] Marathe S, Rao BS, Kumar A. Stabilization of lithomargic soil using cement and randomly distributed waste shredded rubber tyre chips. Int J Eng Trends Technol 2015;23:284–8.
[13] Wang D, Abriak NE, Zentar R. Strength and deformation properties of Dunkirk marine sediments solidified with cement, lime and fly ash. Eng Geol 2013;166:90–9. https://doi.org/10.1016/j.enggeo.2013.09.007.
[14] Shen Z, Cao Y, Fang L. Experimental investigation of rapid stabilization of soft clay soils using chemical admixtures. Soil Mech Found Eng 2017;54:202–10. https://doi.org/10.1007/s11204-017-9459-z.
[15] Moayedi H, Huat BBK, Moayedi F, Asadi A, Parsaie A. Effect of sodium silicate on unconfined compressive strength of soft clay. Electron J Geotech Eng 2011;16 C:289–95.
[16] Ma C, Qin Z, Zhuang Y, Longzhu C, Chen B. Influence of sodium silicate and promoters on unconfined compressive strength of Portland cement-stabilized clay. Soils Found 2015;55:1222–32.
[17] Narendra BS, Sivapullaiah PV, Suresh S, Omkar SN. Prediction of unconfined compressive strength of soft grounds using computational intelligence techniques: A comparative study. Comput Geotech 2006;33:196–208. https://doi.org/10.1016/j.compgeo.2006.03.006.
[18] Zainuddin N, Mohd Yunus NZ, Al-Bared MAM, Marto A, Harahap ISH, Rashid AS, et al. Measuring the engineering properties of marine clay treated with disposed granite waste. Measurement 2019;131:50–60. https://doi.org/10.1016/j.measurement.2018.08.053.
[19] Al-Bared MAM, Marto A, Latifi N. Utilization of recycled tiles and tyres in stabilization of soils and production of construction materials – a state-of-the-art review. KSCE J Civ Eng 2018;22:3860–74. https://doi.org/10.1007/s12205-018-1532-2.
[20] Naeini SA, Rahmani H. Effect of waste bottle chips on strength parameters of silty soil. Int J Civ Environ Eng 2017;11:6–10.
[21] Ilies N, Farcas V, Gherman C, Chiorean V, Popa D. Soils efficient improvement solutions with waste materials and binders. J Environ Prot Ecol 2015;16:1397–406.
[22] Rama Subbarao GV, Siddartha D, Muralikrishna T, Sailaja KS, Sowmya T. Industrial wastes in soil improvement. ISRN Civ Eng 2011;2011:1–5. https://doi.org/10.5402/2011/138149.
[23] Yilmaz F, Kamiloḷlu HA, Şadoḷlu E. Soil stabilization with using waste materials against freezing thawing effect. Acta Phys Pol A 2015;128:392–4. https://doi.org/10.12693/APhysPolA.128.B-392.
[24] Rouaiguia A, El Aal AKA. Enhancement of the geotechnical properties of soils using marble and lime powders, Guelma city. Algeria Geotech Geol Eng 2020;38:5649–65. https://doi.org/10.1007/s10706-020-01368-5.
[25] Saygili A. Use of waste marble dust for stabilization of clayey soil. Mater Sci 2015;21:601–6. https://doi.org/10.5755/j01.ms.21.4.11966.
[26] Sarkar G, Islam R, Alamgir M, Rokonuzzaman M. Interpretation of rice husk ash on geotechnical properties of cohesive soil. Glob J Res Eng Civ Struct Enginering 2012;12:1–7.
[27] Mirzababaei M, Miraftab M, Mohamed M, McMahon P. Unconfined compression strength of reinforced clays with carpet waste fibers. J Geotech Geoenvironmental Eng 2013;139:483–93. https://doi.org/10.1061/(ASCE)GT.1943-5606.0000792.
[28] Li L, Zhang J, Xiao H, Hu Z, Wang Z. Experimental investigation of mechanical behaviors of fiber-reinforced fly ash-soil mixture. Adv Mater Sci Eng 2019;2019:1–10. https://doi.org/10.1155/2019/1050536.
[29] Nazari A, Rajeev P, Sanjayan JG. Modelling of upheaval buckling of offshore pipeline buried in clay soil using genetic programming. Eng Struct 2015;101:306–17. https://doi.org/10.1016/j.engstruct.2015.07.013.
[30] Nguyen MD, Pham BT, Ho LS, Ly HB, Le TT, Qi C, et al. Soft-computing techniques for prediction of soils consolidation coefficient. Catena 2020;195:104802. https://doi.org/10.1016/j.catena.2020.104802.
[31] Kurugodu HV, Bordoloi S, Hong Y, Garg A, Garg A, Sreedeep S, et al. Genetic programming for soil-fiber composite assessment. Adv Eng Softw 2018;122:50–61.
[32] Shahmansouri AA, Akbarzadeh Bengar H, Ghanbari S. Compressive strength prediction of eco-efficient GGBS-based geopolymer concrete using GEP method. J Build Eng 2020;31:101326. https://doi.org/10.1016/j.jobe.2020.101326.
[33] Ly HB, Pham BT, Van Dao D, Le VM, Le LM, Le TT. Improvement of ANFIS model for prediction of compressive strength of manufactured sand concrete. Appl Sci 2019;9:1–16. https://doi.org/10.3390/app9183841.
[34] Momeni E, Yarivand A, Bagher Dowlatshahi M, Jahed Armaghani D. An efficient optimal neural network based on gravitational search algorithm in predicting the deformation of geogrid-reinforced soil structures. Transp Geotech 2020:100446. doi:10.1016/j.trgeo.2020.100446.
[35] Soleimani S, Rajaei S, Jiao P, Sabz A, Soheilinia S. New prediction models for unconfined compressive strength of geopolymer stabilized soil using multi-gen genetic programming. Meas J Int Meas Confed 2018;113:99–107. https://doi.org/10.1016/j.measurement.2017.08.043.
[36] Mozumder RA, Laskar AI, Hussain M. Empirical approach for strength prediction of geopolymer stabilized clayey soil using support vector machines. Constr Build Mater 2017;132:412–24. https://doi.org/10.1016/j.conbuildmat.2016.12.012.
[37] Kalkan E, Akbulut S, Tortum A, Celik S. Prediction of the unconfined compressive strength of compacted granular soils by using inference systems. Environ Geol 2009;58:1429–40. https://doi.org/10.1007/s00254-008-1645-x.
[38] Güllü H, Fedakar Hİ. On the prediction of unconfined compressive strength of silty soil stabilized with bottom ash, jute and steel fibers via artificial intelligence. Geomech Eng 2017;12:441–64. https://doi.org/10.12989/gae.2017.12.3.441.
[39] Cabalar AF, Cevik A, Gokceoglu C. Some applications of adaptive neuro-fuzzy inference system (ANFIS) in geotechnical engineering. Comput Geotech 2012;40:14–33.
[40] Asteris PG, Douvika MG, Karamani CA, Skentou AD, Chlichlia K, Cavaleri L, et al. A novel heuristic algorithm for the modeling and risk assessment of the covid-19 pandemic phenomenon. C - Comput Model Eng Sci 2020;124:1–14. https://doi.org/10.32604/CMES.2020.013280.
[41] Zhou J, Li E, Yang S, Wang M, Shi X, Yao S, et al. Slope stability prediction for circular mode failure using gradient boosting machine approach based on an updated database of case histories. Saf Sci 2019;118:505–18.
[42] Khari M, Dehghanbandaki A, Motamedi S, Armaghani DJ. Computational estimation of lateral pile displacement in layered sand using experimental data. Measurement 2019;146:110–8.
[43] Mohamad ET, Koopialipoor M, Murlidhar BR, Rashiddel A, Hedayat A, Armaghani DJ. A new hybrid method for predicting ripping production in different weathering zones through in-situ tests. Measurement 2019. https://doi.org/10.1016/j.measurement.2019.07.054.
[44] Huang J, Zhang Y, Sun Y, Ren J, Zhao Z, Zhang J. Evaluation of pore size distribution and permeability reduction behavior in pervious concrete. Constr Build Mater 2021;290:123228. https://doi.org/10.1016/j.conbuildmat.2021.123228.
[45] Zhou J, Li X, Shi X. Long-term prediction model of rockburst in underground openings using heuristic algorithms and support vector machines. Saf Sci 2012;50:629–44.
[46] Huang J, Zhang J, Ren J, Chen H. Towards the potential usage of eggshell powder as bio-modifier for asphalt binder and mixture: Workability and mechanical properties. Int J Pavement Eng 2021:1–13. https://doi.org/10.1080/10298436.2021.1905809.
[47] Huang J, Duan T, Zhang Y, Liu J, Zhang J, Lei Y. Predicting the permeability of pervious concrete based on the beetle antennae search algorithm and random forest model. Adv Civ Eng 2020;2020.
[48] Huang J, Sun Y, Zhang J. Reduction of computational error by optimizing SVR kernel coefficients to simulate concrete compressive strength through the use of a

human learning optimization algorithm. Eng Comput 2021. https://doi.org/10.1007/s00366-021-01305-x.
[49] Huang J, Kumar GS, Sun Y. Evaluation of workability and mechanical properties of asphalt binder and mixture modified with waste toner. Constr Build Mater 2021;276:122230.
[50] Huang J, Zhang J, Ren J, Chen H. Anti-rutting performance of the damping asphalt mixtures (DAMs) made with a high content of asphalt rubber (AR). Constr Build Mater 2021;271:121878.
[51] Yang H, Wang Z, Song K. A new hybrid grey wolf optimizer-feature weighted-multiple kernel-support vector regression technique to predict TBM performance. Eng Comput 2020. https://doi.org/10.1007/s00366-020-01217-2.
[52] Zhou J, Asteris PG, Armaghani DJ, Pham BT. Prediction of ground vibration induced by blasting operations through the use of the Bayesian Network and random forest models. Soil Dyn Earthq Eng 2020;139:106390. https://doi.org/10.1016/j.soildyn.2020.106390.
[53] Yang HQ, Li Z, Jie TQ, Zhang ZQ. Effects of joints on the cutting behavior of disc cutter running on the jointed rock mass. Tunn Undergr Sp Technol 2018;81:112–20.
[54] Yang H, Wang H, Zhou X. Analysis on the damage behavior of mixed ground during TBM cutting process. Tunn Undergr Sp Technol 2016;57:55–65.
[55] Liu B, Yang H, Karekal S. Effect of water content on argillization of mudstone during the tunnelling process. Rock Mech Rock Eng 2019. https://doi.org/10.1007/s00603-019-01947-w.
[56] Asteris PG, Cavaleri L, Ly H-B, Pham BT. Surrogate models for the compressive strength mapping of cement mortar materials. Soft Comput 2021. https://doi.org/10.1007/s00500-021-05626-3.
[57] Zhao J, Nguyen H, Nguyen-Thoi T, Asteris PG, Zhou J. Improved Levenberg–Marquardt backpropagation neural network by particle swarm and whale optimization algorithms to predict the deflection of RC beams. Eng Comput 2021. https://doi.org/10.1007/s00366-020-01267-6.
[58] Khandelwal M, Mahdiyar A, Armaghani DJ, Singh TN, Fahimifar A, Faradonbeh RS. An expert system based on hybrid ICA-ANN technique to estimate macerals contents of Indian coals. Environ Earth Sci 2017;76:399. https://doi.org/10.1007/s12665-017-6726-2.
[59] Khandelwal M, Faradonbeh RS, Monjezi M, Armaghani DJ, Majid MZBA, Yagiz S. Function development for appraising brittleness of intact rocks using genetic programming and non-linear multiple regression models. Eng Comput 2017;33:13–21.
[60] Khandelwal M, Singh TN. Evaluation of blast-induced ground vibration predictors. Soil Dyn Earthq Eng 2007;27:116–25.
[61] Armaghani DJ, Asteris PG. A comparative study of ANN and ANFIS models for the prediction of cement-based mortar materials compressive strength. Neural Comput Appl 2020. https://doi.org/10.1007/s00521-020-05244-4.
[62] Asteris PG, Kolovos KG. Self-compacting concrete strength prediction using surrogate models. Neural Comput Appl 2019;31:409–24.
[63] Zhou J, Li X, Mitri HS. Classification of rockburst in underground projects: Comparison of ten supervised learning methods. J Comput Civ Eng 2016;30:4016003.
[64] Zhou J, Li X, Mitri HS. Comparative performance of six supervised learning methods for the development of models of hard rock pillar stability prediction. Nat Hazards 2015;79:291–316.
[65] Murlidhar BR, Armaghani DJ, Mohamad ET. Intelligence prediction of some selected environmental issues of blasting: a review. Open Constr Build Technol J 2020;14:298–308. https://doi.org/10.2174/1874836802014010298.
[66] Momeni E, Yarivand A, Dowlatshahi MB, Armaghani DJ. An Efficient Optimal Neural Network Based on Gravitational Search Algorithm in Predicting the Deformation of Geogrid-Reinforced Soil Structures. Transp Geotech 2020:100446.
[67] Bunawan AR, Momeni E, Armaghani DJ, Rashid ASA. Experimental and intelligent techniques to estimate bearing capacity of cohesive soft soils reinforced with soil-cement columns. Measurement 2018;124:529–38.
[68] Mohamad ET, Armaghani DJ, Momeni E, Abad SVANK. Prediction of the unconfined compressive strength of soft rocks: a PSO-based ANN approach. Bull Eng Geol Environ 2015;74:745–57.
[69] Wang J, Xing Y, Cheng L, Qin F, Ma T. The prediction of mechanical properties of cement soil based on PSO-SVM. 2010 Int Conf Comput Intell Softw Eng CiSE 2010 2010:1–4. doi:10.1109/CISE.2010.5677256.
[70] Huang L, Asteris PG, Koopialipoor M, Armaghani DJ, Tahir MM. Invasive weed optimization technique-based ANN to the prediction of rock tensile strength. Appl Sci 2019;9:5372.
[71] Suman S, Mahamaya M, Das SK. Prediction of maximum dry density and unconfined compressive strength of cement stabilised soil using artificial intelligence techniques. Int J Geosynth Gr Eng 2016;2. doi:10.1007/s40891-016-0051-9.
[72] Dehghanbanadaki A, Khari M, Arefnia A, Ahmad K, Motamedi S. A study on UCS of stabilized peat with natural filler: a computational estimation approach. KSCE J Civ Eng 2019;23:1560–72.
[73] Ray R, Kumar D, Samui P, Roy LB, Goh ATC, Zhang W. Application of soft computing techniques for shallow foundation reliability in geotechnical engineering. Geosci Front 2021;12:375–83. https://doi.org/10.1016/j.gsf.2020.05.003.
[74] Armaghani DJ, Bin Raja RSNS, Faizi K, Rashid ASA. Developing a hybrid PSO–ANN model for estimating the ultimate bearing capacity of rock-socketed piles. Neural Comput Appl 2017;28:391–405.
[75] Pham BT, Qi C, Ho LS, Nguyen-Thoi T, Al-Ansari N, Nguyen MD, et al. A novel hybrid soft computing model using random forest and particle swarm optimization for estimation of undrained shear strength of soil. Sustain 2020;12:1–16. https://doi.org/10.3390/su12062218.
[76] Kutanaei SS, Choobbasti AJ. Prediction of combined effects of fibers and cement on the mechanical properties of sand using particle swarm optimization algorithm. J Adhes Sci Technol 2015;29:487–501. https://doi.org/10.1080/01694243.2014.995343.
[77] Armaghani DJ, Mohamad E, Momeni E, Monjezi M, Sundaram Narayanasamy M. Prediction of the strength and elasticity modulus of granite through an expert artificial neural network. Arab J Geosci 2015;9:1–16. https://doi.org/10.1007/s12517-015-2057-3.
[78] Tian H, Shu J, Han L. The effect of ICA and PSO on ANN results in approximating elasticity modulus of rock material. Eng Comput 2019;35:305–14. https://doi.org/10.1007/s00366-018-0600-z.
[79] Armaghani DJ, Koopialipoor M, Marto A, Yagiz S. Application of several optimization techniques for estimating TBM advance rate in granitic rocks. J Rock Mech Geotech Eng 2019. https://doi.org/10.1016/j.jrmge.2019.01.002.
[80] McCulloch WS, Pitts W. A logical calculus of the ideas immanent in nervous activity. Bull Math Biophys 1943;5:115–33.
[81] Ch S, Mathur S. Particle swarm optimization trained neural network for aquifer parameter estimation. KSCE J Civ Eng 2012;16:298–307.
[82] Simpson PK. Artificial neural systems: foundations, paradigms, applications, and implementations. Pergamon; 1990.
[83] Basheer IA, Hajmeer M. Artificial neural networks: fundamentals, computing, design, and application. J Microbiol Methods 2000;43:3–31. https://doi.org/10.1016/S0167-7012(00)00201-3.
[84] Mohandes MA. Modeling global solar radiation using Particle Swarm Optimization (PSO). Sol Energy 2012;86:3137–45.
[85] Kennedy J, Eberhart RC. A discrete binary version of the particle swarm algorithm. Comput. Cybern. Simulation., 1997 IEEE Int. Conf., IEEE, 1997, p. 4104–4108.
[86] Armaghani DJ, Mohamad ET, Narayanasamy MS, Narita N, Yagiz S. Development of hybrid intelligent models for predicting TBM penetration rate in hard rock condition. Tunn Undergr Sp Technol 2017;63:29–43. https://doi.org/10.1016/j.tust.2016.12.009.
[87] Atashpaz-Gargari E, Lucas C. Imperialist competitive algorithm: an algorithm for optimization inspired by imperialistic competition. Evol. Comput. 2007. CEC 2007. IEEE Congr., IEEE, 2007, p. 4661–7.
[88] Koopialipoor M, Jahed Armaghani D, Hedayat A, Marto A, Gordan B. Applying various hybrid intelligent systems to evaluate and predict slope stability under static and dynamic conditions. Soft Comput 2019;23:5913–29. https://doi.org/10.1007/s00500-018-3253-3.
[89] Koopialipoor M, Fahimifar A, Ghaleini EN, Momenzadeh M, Armaghani DJ. Development of a new hybrid ANN for solving a geotechnical problem related to tunnel boring machine performance. Eng Comput 2019. https://doi.org/10.1007/s00366-019-00701-8.
[90] Bashir ZA, El-Hawary ME. Applying wavelets to short-term load forecasting using PSO-based neural networks. IEEE Trans Power Syst 2009;24:20–7.
[91] Liou SW, Wang CM, Huang YF. Integrative discovery of multifaceted sequence patterns by frame-relayed search and hybrid PSO-ANN. J Univers Comput Sci 2009;15:742–64. https://doi.org/10.3217/jucs-015-04-0742.
[92] Al-Bared MAM, Marto A, Latifi N, Horpibulsuk S. Sustainable improvement of marine clay using recycled blended tiles. Geotech Geol Eng 2018;36:3135–47. https://doi.org/10.1007/s10706-018-0525-8.
[93] Al-Bared MAM, Harahap ISH, Marto A. Sustainable strength improvement of soft clay stabilized with two sizes of recycled additive. Int J GEOMATE 2018;15:39–46.
[94] British Standards Institution. BSI methods of test for soils for civil engineering purposes: part 2. classification tests. London (BS1377); 1990.
[95] British Standards Institution. BSI 1377 methods of test for soils for civil engineering purposes: Part 4, compaction related tests, London, BS1377, Milton Keynes, U.K.; 1990.
[96] BSI 1377: Part 7. British Standard Methods of Test for Soils for Civil Engineering Purposes: Part 7, Shear Strength Tests (Total Stress), BS1377, Milton Keynes, U.K.; 1990.
[97] Hecht-Nielsen R. Kolmogorov's mapping neural network existence theorem. Proc. Int. Conf. Neural Networks, vol. 3, New York: IEEE Press; 1987, p. 11–3.
[98] Mohamad ET, Armaghani DJ, Noorani SA, Saad R, Alvi SV, Abad NK. Prediction of flyrock in boulder blasting using artificial neural network. Electron J Geotech Eng 2012;17:2585–95.
[99] Saghatforoush A, Monjezi M, Faradonbeh RS, Armaghani DJ. Combination of neural network and ant colony optimization algorithms for prediction and optimization of flyrock and back-break induced by blasting. Eng Comput 2016;32:255–66.
[100] Ebrahimi E, Monjezi M, Khalesi MR, Armaghani DJ. Prediction and optimization of back-break and rock fragmentation using an artificial neural network and a bee colony algorithm. Bull Eng Geol Environ 2016;75:27–36.
[101] Zorlu K, Gokceoglu C, Ocakoglu F, Nefeslioglu HA, Acikalin S. Prediction of uniaxial compressive strength of sandstones using petrography-based models. Eng Geol 2008;96:141–58.
[102] Alavi Nezhad Khalil Abad SV, Yilmaz M, Jahed Armaghani D, Tugrul A. Prediction of the durability of limestone aggregates using computational techniques. Neural Comput Appl 2016. doi:10.1007/s00521-016-2456-8.
[103] Jahed Armaghani D, Mohd Amin MF, Yagiz S, Faradonbeh RS, Abdullah RA. Prediction of the uniaxial compressive strength of sandstone using various modeling techniques. Int J Rock Mech Min Sci 2016;85:174–86. https://doi.org/10.1016/j.ijrmms.2016.03.018.

[104] Pourakbar S, Asadi A, Huat BBK, Fasihnikoutalab MH. Stabilization of clayey soil using ultrafine palm oil fuel ash (POFA) and cement. Transp Geotech 2015;3:24–35. https://doi.org/10.1016/j.trgeo.2015.01.002.

[105] Etim RK, Eberemu AO, Osinubi KJ. Stabilization of black cotton soil with lime and iron ore tailings admixture. Transp Geotech 2017;10:85–95. https://doi.org/10.1016/j.trgeo.2017.01.002.

[106] Sumayya K, Rafeequedheen KM, Sameer V, Firoz, Khais P, Jithin K. Stabilization of expansive soil treated with tile waste. Int J Civ Eng 2016;3:67–75. doi:10.14445/23488352/ijce-v3i3p112.